OXFORD

Temporal dynamics of white and gray matter plasticity during motor skill acquisition: a comparative diffusion tensor imaging and multiparametric mapping analysis

Tim Emmenegger [1], Gergely David[1], Siawoosh Mohammadi[2,3,4], Gabriel Ziegler[5,6], Martina F. Callaghan[7], Alan Thompson[8],

Karl J. Friston[7], Nikolaus Weiskopf[3,7,9], Tim Killeen [1], Patrick Freund [1,7,*]

[1]Spinal Cord Injury Center, Balgrist University Hospital, University of Zurich, Forchstrasse 380, 8008 Zürich, Switzerland
[2]Max Planck Research Group MR Physics, Max Planck Institute for Human Development, Lentzeallee 9414195 Berlin, Germany
[3]Department of Neurophysics, Max Planck Institute for Human Cognitive and Brain Sciences, Stephanstraße 1AD-04103 Leipzig, Germany
[4]Department of Neuroradiology, University Hospital Schleswig-Holstein and University of Lübeck, Ratzeburger Allee 16023538 Lübeck, Germany
[5]Institute of Cognitive Neurology and Dementia Research, Otto-von-Guericke-University Magdeburg, Leipziger Str. 44, 39120 Magdeburg, Germany
[6]German Center for Neurodegenerative Diseases (DZNE), Leipziger Str. 44/Haus 64, 39120 Magdeburg, Germany
[7]Wellcome Centre for Human Neuroimaging, UCL Queen Square Institute of Neurology, University College London, 12 Queen Square, London WC1N 3AR, United Kingdom
[8]Department of Neuroinflammation, UCL Institute of Neurology, University College London, Gower Street, London, WC1E 6BT, United Kingdom
[9]Felix Bloch Institute for Solid State Physics, Faculty of Physics and Earth System Sciences, Leipzig University, Linnéstraße 5, 04103 Leipzig, Germany

*Corresponding author: Patrick Freund, Spinal Cord Injury Center, Balgrist University Hospital, University of Zurich, Forchstrasse 380, CH8008 Zurich, Switzerland.
E-mail: patrick.freund@balgrist.ch

Learning new motor skills relies on neural plasticity within motor and limbic systems. This study uniquely combined diffusion tensor imaging and multiparametric mapping MRI to detail these neuroplasticity processes. We recruited 18 healthy male participants who underwent 960 min of training on a computer-based motion game, while 14 were scanned without training. Diffusion tensor imaging, which quantifies tissue microstructure by measuring the capacity for, and directionality of, water diffusion, revealed mostly linear changes in white matter across the corticospinal-cerebellar-thalamo-hippocampal circuit. These changes related to performance and reflected different responses to upper- and lower-limb training in brain areas with known somatotopic representations. Conversely, quantitative MRI metrics, sensitive to myelination and iron content, demonstrated mostly quadratic changes in gray matter related to performance and reflecting somatotopic representations within the same brain areas. Furthermore, while myelin and iron-sensitive multiparametric mapping MRI was able to describe time lags between different cortical brain systems, diffusion tensor imaging detected time lags within the white matter of the motor systems. These findings suggest that motor skill learning involves distinct phases of white and gray matter plasticity across the sensorimotor network, with the unique combination of diffusion tensor imaging and multiparametric mapping MRI providing complementary insights into the underlying neuroplastic responses.

Key words: plasticity; dMRI; DTI; hippocampus; motor system.

Introduction

Acquiring new complex motor skills, such as dancing or juggling, requires both physical and cognitive effort and induces structural and functional changes across cortical and subcortical brain areas (Boyke et al. 2008; Draganski and May 2008; Scholz et al. 2009; Dayan and Cohen 2011; Hüfner et al. 2011; Taubert et al. 2011, 2016; Reid et al. 2017; Jacobacci et al. 2020; Azzarito et al. 2023). Multiparametric mapping (MPM; Weiskopf et al. 2021)— a quantitative MRI (qMRI) technique sensitive to myelin and iron content changes—revealed evidence of performance-related, microstructural changes across a corticospinal-cerebellar-thalamo-hippocampal circuit in healthy controls during a motor task (Azzarito et al. 2023). This system has been shown to be involved in the acquisition and refinement of motor skills through practice and experience (Boyke et al. 2008; Taubert et al. 2010; Zatorre et al. 2012; Kodama et al. 2018; Azzarito et al. 2023). Within this circuit, the corticospinal tract is the major

pathway, originating from the premotor and supplementary motor areas where motor commands are generated (Lemon and Morecraft 2023). The cerebellum is responsible for adjusting and refining these motor outputs to produce smooth, accurate, and coordinated movements. It processes sensory information from muscles and joints and adapts motor plans from the cerebral cortex (Manto et al. 2015). The flow of this information between the cerebellum and cerebral cortex is regulated by the thalamus, which ensures coordinated and timely movements (Prevosto and Sommer 2013; La Terra et al. 2022). Meanwhile, the hippocampal formation aids in the creation of new memories associated with motor tasks, as well as spatial memory and navigation, which are essential for complex motor skills (Leutgeb et al. 2005; Kodama et al. 2018). Crucially, myelin changes in the sensorimotor system preceded those in the hippocampal formation and conformed anatomically to the known somatotopic representation within the internal

capsule, after upper- and lower-limb training (Azzarito et al. 2023).

The specificity of MPM may be complemented and improved upon through combination with other imaging techniques, including diffusion tensor imaging (DTI), which is highly sensitive to the rate and directionality of water movement within white matter (Basser et al. 1994; Seiler et al. 2021; Chen et al. 2024). DTI furnishes metrics for white matter (WM) structures, allowing the assessment of myelin and axonal changes in vivo (Scholz et al. 2009; Beaulieu 2011; Martin et al. 2016; David et al. 2019). It has also proven sensitive to changes in gray matter (GM) microstructure, where increases in mean diffusivity (MD) have been observed in diseases such as frontotemporal dementia, semantic dementia, progressive nonfluent aphasia, and Alzheimer's disease (Whitwell et al. 2010; Weston et al. 2015). Additionally, DTI has revealed significantly higher fractional anisotropy (FA), axial diffusion (AD), and lower radial diffusion (RD) values within major fiber tracts in professional athletes and musicians, compared to healthy non-professionals, indicating fiber tract reorganization and/or increases in WM integrity (Bengtsson et al. 2005; Johansen-Berg et al. 2007; Han et al. 2009; Wang et al. 2013; Pi et al. 2019). Moreover, DTI has captured dynamic changes within WM during the acquisition of new motor skills, such as juggling or finger tapping (Scholz et al. 2009; Takeuchi et al. 2010; Hofstetter et al. 2013; Reid et al. 2017). There is no doubt that such studies provide evidence for the value of using DTI to detect neuroplasticity in learning motor tasks. However, their transferability to a clinical environment is hindered, as most previously chosen motor tasks are inappropriate for clinical rehabilitation practice, as discussed in our previous publication (Azzarito et al. 2023). In contrast, tasks such as arm reaching or lower-limb functions are of greater importance in most neurological conditions (Mayo et al. 2002; Roby-Brami et al. 2003; Lum et al. 2009; Patterson et al. 2011; Simpson et al. 2012; Chen et al. 2015).

In this study, we investigate training-induced plasticity in the brains of healthy male individuals using DTI, focusing on a challenging yet achievable task suited to subjects with and without neurological impairments (Prahm et al. 2017; Azzarito et al. 2023). Healthy young to middle-aged male subjects were recruited for this study due to the higher prevalence of men affected by traumatic spinal cord injury (Jackson et al. 2004), which is the therapeutic target of the training intervention under investigation. This approach enhances our capability to understand rehabilitation changes in the majority of these patients. Through a series of longitudinal MRI scans—acquired before, during, and after the training—our study pursues several inter-related objectives: (i) understanding the spatiotemporal changes in DTI metrics induced by training in subcortical and cortical areas, which accompany the acquisition of motor skills; (ii) investigating specific somatotopic changes related to training the upper versus lower limbs; (iii) exploring correlations between DTI changes and improvements in performance; (iv) ascertaining which components of the motor system respond earliest to training; and (v) contextualizing DTI findings with the microstructural changes documented in the multiparametric mapping MRI study by Azzarito et al. 2023.

Materials and methods
Participants
This study was conducted with the same individuals undergoing the motor training paradigm described in Azzarito et al. (2023), where the inclusion of spinal cord injury patients is planned. Recruitment for this study was limited to males due to the higher prevalence of men affected by (incomplete) traumatic spinal cord injury: the therapeutic target of the training intervention under investigation. A total of 32 healthy adult males, all right-handed, were recruited for the study, with age spanning from 23 to 62 years (for additional demographic information see Supplementary Table 1). These participants were recruited into three training groups: an upper-limb training group ($n = 9$), a lower-limb training group ($n = 9$), and a no-training group ($n = 14$). The initial six participants were assigned to the upper, lower, or no-training groups through block randomization. Subsequently, an age-matching algorithm was applied to ensure that the composition of the participant group closely resembled the demographic profile of typical spinal cord injury patients; specifically young to middle-aged individuals (Jackson et al. 2004). This approach was adopted to ensure applicability to patient cohorts in future studies. All participants had either normal or corrected to normal vision, had no prior history of psychological or neurological disorders, showed no contraindications for MRI, and were unfamiliar with the experimental procedures.

Training task
Participants engaged in motor training for four consecutive weeks, with four 60-min training sessions per week (Fig. 1A). After this training phase, participants were prohibited from further task-related training between day 28 and day 84. On day 84, an evaluation of performance retention was carried out. Control participants did not undergo training or performance assessments. All participants were instructed not to acquire new behavioral skills or participate in dance classes during the study but to maintain their regular daily routines. Furthermore, none of the study participants were allowed to take any dance lessons, and none of the participants are or were professional dancers. However, we did not assess whether the participants had ever taken dance lessons in the past.

The motor training task is described in more detail in Azzarito et al. (2023). In short, subjects were trained to match scrolling arrow symbols on a screen ($\leftarrow \uparrow \rightarrow \downarrow$) by activating corresponding panels on the input device synchronized with popular songs played from the speakers. The participant was tasked with selecting and activating the correct symbol at the precise moment the scrolling arrow overlapped with a set of static arrows at the top of the screen (Supplementary Video 1). The moment of overlap was synchronized to the beat of the music using the Dancing Monkeys script (Karl O'Keeffe, https://monket.net/dancing-monkeys/). The script generates patterns of arrows of varying difficulty while excluding sequences that would be impossible to respond to. After each bout, lasting 120 s, the participant received immediate visual feedback in the form of a percentage score (accurate response within 45 ($\pm$ 22.5 ms) ms: 2 points, 45 to 90 ms: 1 point, >90 ms: no score; cumulative score expressed as a percentage of the maximum possible points). To avoid rote learning of a series of movements, the pattern of arrows differed for each bout, and participants improved by developing optimal strategies for adapting to the varying patterns (Orrell et al. 2006). The optimal response involved identifying and executing multistep responses to frequently encountered patterns of arrows as they were revealed. Each training session comprised 15 bouts, with ~120 s of rest between each. Progress in the training involved moving through increasingly difficult levels, with the number, pattern complexity, and scroll speed of the arrows increasing. The next level was unlocked when three non-consecutive scores of $\geq$80% were achieved within a level. Demotion to the previous level was mandated by three consecutive scores of $\leq$30%.
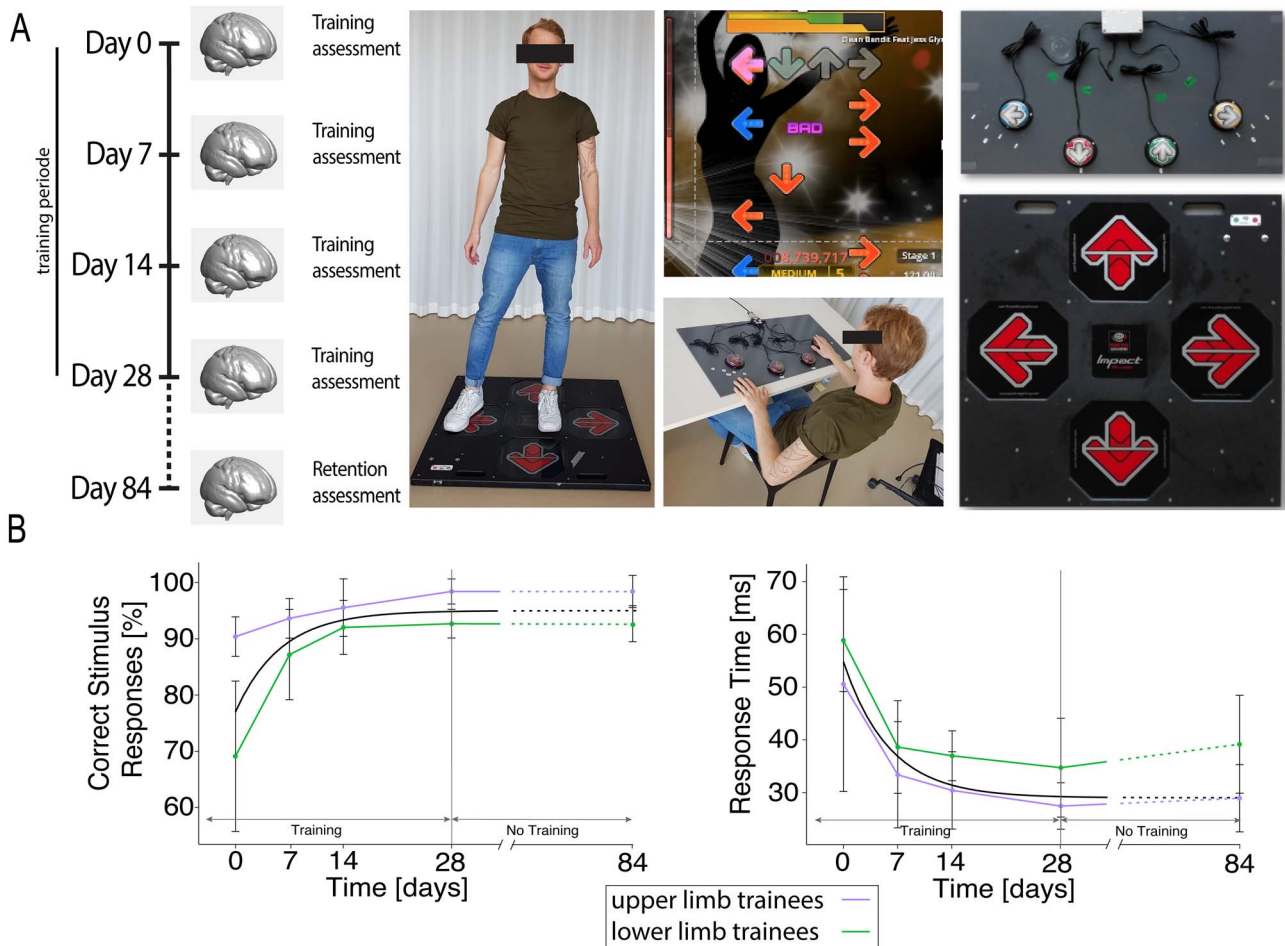
Fig. 1. Experimental design, training task, and behavioral data. The experimental design (A) involved MRI acquisition and training assessments at baseline (day 0), during the training period (days 7, 14, and 28), and at the final retention assessment (day 84). Participants completed 60 min of supervised training in a motor skill task four times per week for four consecutive weeks, activating inputs with their hands or feet (depending on whether they were allocated to the upper or lower limb training groups) in response to rhythmic aural and visual stimuli in the dance game StepMania. Behavioral improvement, defined as the percentage of correct stimulus responses, and response time (correctly pressed button within 90 ms of the cue being presented) were measured during a formal, standardized performance test at weekly intervals. (B) Median values for these metrics are plotted with interquartile range. The dashed lines connect the last training point (day 28) with the retention test on day 84.

For upper- and lower-limb training, we employed StepMania 5 Beta 3 software (available at www.stepmania.com) for Windows 7 (Microsoft, La Jolla, CA). In addition to the software, specific input devices tailored to the targeted limbs were utilized.

Participants in the lower-limb training group used a dance platform (Impact Dance Platform; Positive Gaming BV, Haarlem, Netherlands) as their input device. This setup allowed them to effectively learn to "dance" in response to the arrow stimuli, as shown in Fig. 1A. Meanwhile, participants in the upper-limb training group used a custom-made platform designed to emulate the lower-limb platform, depicted in Fig. 1A. Participants were instructed to employ their left hand for ← and ↑ inputs and their right hand for → and ↓ inputs.

Formal evaluation of task performance—for correlation with MRI metrics—was performed at baseline (prior to training) and on days 7, 14, 28, and 84. These assessments used predetermined arrow patterns of increasing complexity and included segments at increasing tempos (60, 80, 100, and 120 beats per minute). To prevent rote learning, arrow patterns were different at each assessment timepoint but complexity was standardized using the Dancing Monkeys script (Karl O'Keeffe, https://monket.net/dancing-monkeys/). All participants undertook identical

performance assessments. The total duration of this assessment was 3 min and 20 s.

Behavioral analyses

As in Azzarito et al. (2023), performance was measured in terms of the percentage of correct stimulus responses (%CSR) and response time (RT). %CSR was defined as the percentage of correct inputs within 90 ms of the cue, while RT represented the mean absolute ± delay in milliseconds between overlap of timing of cue and arrow on the top row cue overlap and the time of correct inputs. To quantify behavioral improvement, we employed customized Matlab 2016b (The MathWorks, Natick, MA, USA) routines.

An exponential model of $y = \alpha - \delta\, e^{-\gamma t} + \varepsilon$ was fitted to measured performance improvement over the training period t (baseline, days 7, 14, and 28), where y represents the performance parameter (%CSR or RT), α the asymptote of the curve (the learning plateau), δ the acquisition climb or the extent of improvement from baseline to asymptote, and γ the time needed to reaching the asymptote (speed in improving). The error term ε was assumed to be normally distributed with a mean of 0. These parameters were estimated individually for each participant, and separately

for left- and right-sided responses using MATLAB's custom non-linear census fitting function. Parameters δ and γ were analyzed to investigate several aspects of sensorimotor learning: (i) skill acquisition across all participants, (ii) disparities between upper- and lower-limb training, (iii) differences between left and right lateralized training responses, and (iv) MRI correlates. The first three aspects were assessed using Stata 15.0 (Stata Corp, College Station, TX), while the fourth was assessed using SPM (Statistical Parametric Mapping version 12 v7487; https://www.fil.ion.ucl.ac.uk/spm).

To evaluate the normality of performance parameters (δ and γ), the Shapiro–Wilk test was employed. Differences in performance between upper- and lower-limb training were assessed using a two-sample Wilcoxon rank-sum test on the γ and δ values of all trained participants. Lastly, to determine if the acquired skill was retained at follow-up, a Wilcoxon matched-pairs signed-rank test was conducted on %CSR and RT at days 28 and 84.

MRI acquisition

All MRI measurements were acquired using a 3-T Siemens Skyra[fit] scanner (Siemens Healthcare, Erlangen, Germany) with a 16-channel receive head and neck coil, and employing Syngo MR E11 software. Scans were performed at five timepoints, including baseline (prior to training) and on days 7, 14, and 28, as well as at 84-day follow-up. When both scanning and training were scheduled for the same day, the training was conducted after the scan. At each timepoint, we acquired a diffusion MRI (dMRI) dataset for DTI and a multiparameter mapping (MPM) protocol for quantitative maps (for details please see Azzarito et al. 2023).

The dMRI dataset comprised 60 diffusion-weighted images with a *b*-value of 1200 s/mm^2, each employing a unique diffusion-encoding direction, and 7 T2-weighted images with a *b*-value of 0 s/mm^2. These scans were obtained using a 2D single-shot spin-echo echo-planar imaging sequence that covered the entire brain. The sequence included 56 slices with a thickness of 2.5 mm and a 10% gap, acquired in an ascending interleaved order. Additional acquisition parameters were as follows: in-plane resolution of 2.5×2.5 mm^2, in-plane field of view measuring 220×220 mm^2, repetition time of 7600 ms, echo time of 80 ms, flip angle of 90°, GRAPPA (generalized autocalibrating partially parallel acquisition) with an acceleration factor of 2 in the phase-encoding direction (anterior–posterior), 7/8 phase partial Fourier, nominal echo spacing of 0.7 ms, and readout bandwidth of 1624 Hz/pixel, for a total dMRI acquisition time of 8 min and 54 s. Additionally, a single, T2-weighted image with a *b*-value of 0 s/mm^2, sharing the same geometry and sequence parameters but featuring an opposite phase-encoding direction (posterior–anterior), was acquired. For comprehensive details of the MPM protocol, please refer to Azzarito et al. (2023).

MRI processing

The dMRI dataset underwent several processing steps. First, denoising was applied using the MRtrix3 package (www.mrtrix.org). Subsequently, the data underwent eddy-current and motion correction using *eddy* and susceptibility distortion correction using *topup* (FSL version 5.0.11). A weighted least squares algorithm was employed to generate maps of DTI metrics including FA, MD, AD, and RD. These DTI maps were then co-registered to the magnetization saturation transfer (MT$_{sat}$) map derived from the MPM protocol. To normalize the co-registered DTI maps to the MNI152 template, the forward deformation field (native to template space) obtained from the MPM protocol, as described in Azzarito et al. (2023), was applied. In obtaining these deformation fields, the MT$_{sat}$ maps

were first skull-stripped. For skull-stripping, the MT$_{sat}$ maps were segmented using the "Segment Longitudinal Data" function of the CAT12 toolbox (CAT12.6 (r1450), http://www.neuro.uni-jena.de/cat/) with the graph-cut/region-growing approach. After this skull-stripping step, the MT$_{sat}$ maps were used for longitudinal registration within participants, based on a generative model. In this model, each map was registered to a subject-specific average map, combining nonlinear and rigid-body registration with corrections for intensity bias artifacts (Ashburner 2013). This procedure generated participant-specific midpoint maps with corresponding deformation fields. Second, a unified segmentation was applied to the subject's midpoint map, generating probability maps of GM, WM, and cerebrospinal fluid (Ashburner and Friston 2005). Third, nonlinear template generation and image registration were applied to subject-specific midpoint GM and WM tissue maps based on Dartel (Ashburner 2007), and the resulting template was registered to Montreal Neurological Institute (MNI) space using an affine transform.

Spatial smoothing was applied to the DTI maps, using a tissue-specific 5 mm full-width at half-maximum Gaussian kernel within both the GM and WM, following the methodology outlined in Draganski et al. (2011). For comprehensive details regarding the pre-processing of the qMRI, please refer to Azzarito et al. (2023). It should be noted that MD was analyzed only in the GM, while FA, RD, and AD were analyzed exclusively in the WM.

Statistical analyses
Regions of interest

Our DTI approach encompassed three components: (i) an explorative whole-brain analysis, (ii) a hypothesis-driven region of interest (ROI) analysis, and (iii) analysis of coherent patterns of changes across ROIs and over time. The selected ROIs for our analysis included regions identified as key to sensorimotor learning; the sensorimotor cortices [including motor cortex areas 4a and 4p and primary somatosensory cortex areas 3a, 3b, 1, and 2 from the Anatomy Toolbox of SPM (Eickhoff et al. 2005, 2007)], cranial corticospinal tract (CST, including the regions of the medulla oblongata, cerebral peduncle, internal capsule, and superior corona radiata from the ICBM-DTI-81 white-matter labels atlas available from FSL, https://fsl.fmrib.ox.ac.uk), thalamus [Oxford thalamic connectivity atlas available from the Anatomy Toolbox of SPM (Eickhoff et al. 2005, 2007) and FSL], cerebellum [available from the Anatomy Toolbox of SPM and FSL (Eickhoff et al. 2005, 2007; Diedrichsen 2006)], and hippocampal formations [including areas of the cornu ammonis 1, 2, and 3, dentate gyrus, entorhinal cortex, and subiculum available from the Anatomy Toolbox of SPM (Eickhoff et al. 2005, 2007)]. These choices were grounded in previous studies that reported GM and WM changes in response to upper- and lower-limb training (Draganski et al. 2006; Boyke et al. 2008; Scholz et al. 2009; Hüfner et al. 2011; Schlegel et al. 2012; Lakhani et al. 2016; Wenger et al. 2016; Kodama et al. 2018; Long et al. 2018; Azzarito et al. 2023). For each hemisphere and tissue type (GM and WM), we defined a single ROI. The ROI definitions for the CST were based on the FSL templates in MNI space. Meanwhile, the sensorimotor cortex, thalamus, hippocampal formation, and cerebellum were defined using the anatomy toolbox in SPM, as detailed in Eickhoff et al. (2005, 2007).

Training-induced structural changes

We employed SPM to examine (i) training-induced brain changes, (ii) somatotopic effects, and (iii) the relationship between training performance and structural adaptation. To compare the changes

in DTI metrics with those in qMRI metrics observed in Azzarito et al. (2023), we conducted a mass-univariate approach for each parameter and superimposed the significant results of the training response, as outlined in Draganski et al. (2011).

For modeling training-induced brain changes, we employed a general linear model within SPM, which incorporated linear and quadratic terms, as well as an intercept, for each subject. Age and total intracranial volume (TIV) were included as covariates in the model for each subject. This approach allowed us to estimate the DTI parameter changes individually and can be used to associate the linear or quadratic changes with the subjects' improvements. The linear and quadratic terms were mean-centered, and the linear component was orthogonalized with respect to the quadratic component. This orthogonalization enabled us to identify both linear and transient negative quadratic (increase–decrease) and transient positive quadratic (decrease–increase) trajectories, following the methodology described in Ziegler et al. (2018). The use of this second-order polynomial regression is important because the quadratic terms model early and late phases that can have opposite signs: e.g. plastic changes in the neuropil followed by myelination, or early changes that then revert to baseline (see discussion).

Training-induced brain changes were defined as the difference in the quadratic model parameters between the combined trained group (comprising upper- and lower-limb training) and the untrained group. The same model was used to assess somatotopic effects by comparing lower-limb with upper-limb trainees within the same ROIs. Therefore, it would be expected that neuroplastic changes from the upper-limb trainees would occur in different subareas of the same brain structures that have somatotopic representation, compared to the lower-limb trainees.

To characterize MRI correlates of motor learning, we used SPM's multiple linear regression models. We examined the associations of the linear and quadratic terms of the quadratic model with improvements in performance. Specifically, we assessed associations at the baseline prior to training (α–δ), with training-induced behavioral improvement (δ), and with the speed of improvement (γ). To ensure the robustness of our inferences, we included only subjects whose behavioral parameters fell within 3 SD of the group mean, thus mitigating the influence of outliers. Significant clusters were identified after applying a conservative cluster-forming threshold of $P = 0.001$ All results were subjected to family-wise error (FWE) correction ($P < 0.05$), and a cluster size of ≥ 20 voxels was considered significant.

Assessment of retention of training-induced microstructure changes

To evaluate the retention of training-induced microstructural changes, we computed the mean values of FA, MD, AD, and RD within clusters that had exhibited significant responses to training in each participant from the last 2 timepoints (i.e. days 28 and 84). Subsequently, we conducted frequency and probability testing to assess significant differences and the probability of equivalence between the trained and untrained individuals on day 84. For this analysis, we employed the Welch two-sample t-test in RStudio (version 2022 July 1) and the Bayesian independent-samples t-test in JASP (version 0.17.1). Similarly, we explored significant differences and the probability of equivalence within the trained group between day 28 and day 84. To categorize the strength of the evidence for equivalence, we used the classification system proposed by Kass and Raftery (1995).

Coherent changes in microanatomy within the motor system

To characterize coherent changes in distinct brain regions—which may involve concurrent changes in different regions at the same time or time-lagged changes at subsequent timepoints—we calculated the mean for each DTI metric from the significant (group comparison) clusters in MNI space for all trained participants, as discussed above in Section "Training-induced structural changes". For the time-lagged analyses, we employed a mixed-effects model to investigate correlations between mean MRI parameters in one cluster at a specific timepoint and the same parameter in another cluster at the subsequent timepoint (including baseline, days 7, 14, and 28), corrected for age and TIV. This analysis focused specifically on the motor system, encompassing the corticospinal tract and cerebellum, with the aim of exploring the sequence of responses within the motor system to training. Specifically, we sought to identify correlations between changes in one cluster (for example, mean FA from the left corticospinal tract) and time-lagged changes in another cluster (for example, mean FA from the right cerebellum at the subsequent timepoint). This can be regarded as a simple form of directed functional connectivity analysis (Friston et al. 2013), of the sort used to establish Granger causality based upon temporal precedence; i.e. a statistical dependency between measures in one region and preceding measures in another. Finally, we tested for coherent changes between paired brain structures in the contralateral hemisphere at the same timepoint.

Approvals, registrations, and participant consents

The study was conducted in compliance with Good Clinical Practice and the Declaration of Helsinki and received approval from the Zurich Cantonal Ethics Committee (KEK-2013-0559). Written informed consent was obtained from all participants.

Data availability

Anonymized grouped data may be shared upon request by a qualified investigator.

Results
Demographics and behavioral results

The groups did not significantly differ with respect to age. All trained participants improved (in terms of δ) in both %CSR and RT over 28 days of training (%CSR: lower limb median = 22% [interquartile range, IQR: 22% to 29%], upper limb median = 11% [IQR: 9% to 12%], $P = 0.004$, two-tailed test; RT: median = 30.05 ms [IQR: 13.8 to 34.82 ms], upper limb median = 25.4% [IQR: 22.58 to 28.4 ms], $P = 0.895$). The median number of days to reach 95% of their maximal improvement, computed as $3/\gamma$, was 18 (%CSR: lower limb 14 days median $\gamma = 0.22$ [IQR: 0.21 to 0.29], upper limb 27 days median $\gamma = 0.11$ [IQR: 0.09 to 0.19], $P = 0.190$, two-tailed test; RT: lower limb 15 days median $\gamma = 0.20$ [IQR: 0.09 to 0.28], upper limb 21 days median $\gamma = 0.14$ [IQR: 0.11 to 0.27], $P = 0.796$; Fig. 1B and Azzarito et al. 2023). At baseline, no significant difference in RT between lower-limb trainees (58.8 ms) and upper-limb trainees (50.6 ms) was found ($P = 0.171$). Nevertheless, upper-limb trainees (%CSR) achieved a significantly higher %CSR at baseline compared to lower-limb trainees (90.4% vs. 69.1%, $P = 0.001$). This resulted in a significantly higher improvement in terms of %CSR in lower-limb trainees compared to upper-limb

trainees (22% vs. 11%, $P = 0.004$), while improvement in terms of RT was not significantly different (lower limb: 30.1 ms, upper limb: 25.4 ms, $P = 0.895$). As previously described, specific improvements in %CSR and RT for inputs exclusively delivered by the left or right side were not significantly different ($P > 0.05$, two-tailed test), nor were significant differences in %CSR and RT observed (%CSR lower limb $P = 0.910$, upper limb $P = 0.531$; RT lower limb $P = 0.100$, upper limb $P = 0.652$) between days 28 (lower limb: %CSR = 92.68% [IQR: 91.08% to 93.63%], RT = 38.57 ms [IQR: 34.73 to 46.97 ms]; upper limb: %CSR = 98.41% [IQR: 97.45% to 99.68%], RT = 29.05 ms [IQR: 27.08 to 38.64 ms]) and 84 days (lower limb: %CSR = 92.67% [IQR: 90.76% to 93.97%], RT = 41.84 ms [IQR: 39.17 to 52.33 ms]; upper limb: %CSR = 98.41% [IQR: 97.13% to 100.00%], RT = 30.24 ms [IQR: 25.92 to 34.87 ms]).

Microstructural responses to training
Whole-brain analysis

At baseline, no significant differences in any DTI metrics were observed between the trained and non-trained groups. During training, utilizing an exploratory whole-brain approach for GM and WM analysis (Supplementary Fig. 1 and Supplementary Table 2), we observed linear increases in FA and AD, as well as linear decreases in RD and MD in the trained group compared to the non-trained group across various brain regions. Specifically, significant differences in the linear change were found in the bilateral cerebellum (left: FA: $z = 4.493$, $P < 0.001$; AD: $z = 4.665$, $P < 0.001$; RD: $z = 4.569$, $P < 0.001$; MD: $z = 4.481$, $P < 0.001$; right: FA: $z = 4.378$, $P < 0.001$; AD: $z = 3.978$, $P = 0.028$; MD: $z = 4.705$, $P < 0.001$), the corona radiata near the motor cortex (RD: $z = 5.682$, $P = 0.034$), WM in the vicinity of the left hippocampus (FA: $z = 4.376$, $P = 0.002$; AD: $z = 4.790$, $P < 0.001$), and the WM within the brainstem (right: RD: $z = 4.535$, $P < 0.001$; left RD: $z = 3.982$, $P = 0.015$) (Supplementary Fig. 1 and Supplementary Table 2). Furthermore, trainees exhibited greater negative quadratic changes in FA and greater positive quadratic changes in RD in the corpus callosum (FA: $z = 4.479$, $P = 0.033$; RD: $z = 4.265$, $P = 0.037$) and the left corona radiata (FA: $z = 4.118$, $P = 0.008$; RD: $z = 4.258$, $P = 0.001$; Supplementary Table 2).

ROI-based analysis

At baseline, no differences were found between trainees and non-trainees for any MRI metric or ROI. In response to training, trainees exhibited greater positive linear changes in FA, AD, and RD, compared to non-trained participants, in the WM of the cerebellum (left: FA: $z = 4.870$, $P < 0.001$, AD: left: $z = 4.901$, $P < 0.001$; right: FA: $z = 4.356$, $P < 0.001$, AD: $z = 4.075$, $P < 0.001$) and corticospinal tract (left: FA: $z = 3.962$, $P = 0.009$, AD: $z = 3.993$, $P = 0.042$, RD: $z = 4.746$, $P < 0.001$; right FA: $z = 4.354$, $P = 0.029$, RD: $z = 4.509$, $P < 0.001$) (Table 1, Fig. 2, and Supplementary Fig. 2). Moreover, trainees showed greater negative linear changes in MD compared to non-trained participants in the GM of the cerebellum (left: $z = 5.198$, $P < 0.001$; right: $z = 4.813$, $P < 0.001$), thalamus (left: $z = 4.366$, $P = 0.002$; right: $z = 4.460$, $P < 0.001$), and hippocampus ($z = 4.668$, $P < 0.001$; Table 1, Fig. 2, and Supplementary Fig. 2). Overall, training-induced microstructural changes occurred in both cortical and subcortical structures, involving both GM and WM.

Associations with performance improvements
Whole-brain analysis

We found a positive correlation between linear changes in FA and AD in the left corona radiata inferior to the sensorimotor cortices

Table 1. Longitudinal statistical parametric mapping (SPM) demonstrated differences in the linear time dependence of fractional anisotropy (FA), axial diffusivity (AD), radial diffusivity (RD), and mean diffusivity (MD) maps between trainees and untrained subjects. To compare the differences at day 84 between trained and non-trained subjects, as well as the difference between days 28 and 84 for the trained subjects, the mean cluster of the linear changes was extracted and analyzed using Welch's t-test and Bayesian statistics. The Bayes factor (BF_{01}) is reported, where a value > 1 indicates a preference for the null (H_0) hypothesis. R = right, L = left.

| ROI	MAP	Contrast	P-value (FWE-corrected)	Cluster size	z-Value	x (mm)	y (mm)	z (mm)	Trained vs non-trained at day 84 P-value	Trained vs non-trained at day 84 BF_{01}	Trained day 28 vs 84 d P-value	Trained day 28 vs 84 d BF_{01}
Cerebellum WM L	FA	lin trained > NonTrained	0.000	475	4.870	−28.5	−49.5	−37.5	0.691	2.746	0.189	1.848
Corticospinal tract WM L	FA	lin trained > NonTrained	0.009	76	3.962	−9.0	−28.5	−15.0	0.517	2.429	0.390	2.923
Cerebellum WM R	FA	lin trained > NonTrained	0.000	374	4.356	15.0	−46.5	−30.0	0.543	2.509	0.377	2.864
Corticospinal tract WM R	FA	lin trained > NonTrained	0.029	55	4.354	6.0	−27.0	−13.5	0.375	2.023	0.563	3.524
Cerebellum WM L	AD	lin trained > NonTrained	0.000	513	4.901	−28.5	−46.5	−37.5	0.260	2.023	0.096	1.140
Corticospinal tract WM L	AD	lin trained > NonTrained	0.042	48	3.993	−7.5	−25.5	−12.0	0.865	2.919	0.298	2.492
Cerebellum WM R	AD	lin trained > NonTrained	0.000	230	4.075	10.5	−57.0	−31.5	0.186	1.318	0.441	3.124
Corticospinal tract WM L	RD	lin trained < NonTrained	0.000	584	4.746	−25.5	−49.5	−36.0	0.341	1.890	0.369	2.832
Corticospinal tract WM R	RD	lin trained < NonTrained	0.000	628	4.509	9.0	−33.0	−15.0	0.096	0.715	0.794	3.986
Cerebellum GM L	MD	lin trained < NonTrained	0.000	951	5.198	−9.0	−88.5	−31.5	0.145	1.082	0.497	3.321
Thalamus GM L	MD	lin trained < NonTrained	0.002	170	4.366	0.0	−22.5	−7.5	0.508	2.500	0.722	3.879
Cerebellum GM R	MD	lin trained < NonTrained	0.000	1146	4.813	22.5	−69.0	−21.0	0.494	2.395	0.122	1.362
Hippocampus GM R	MD	lin trained < NonTrained	0.000	238	4.668	30.0	−42.0	−3.0	0.103	0.826	0.651	3.742
Thalamus GM R	MD	lin trained < NonTrained	0.000	220	4.460	6.0	−31.5	−3.0	0.268	1.746	0.162	1.661
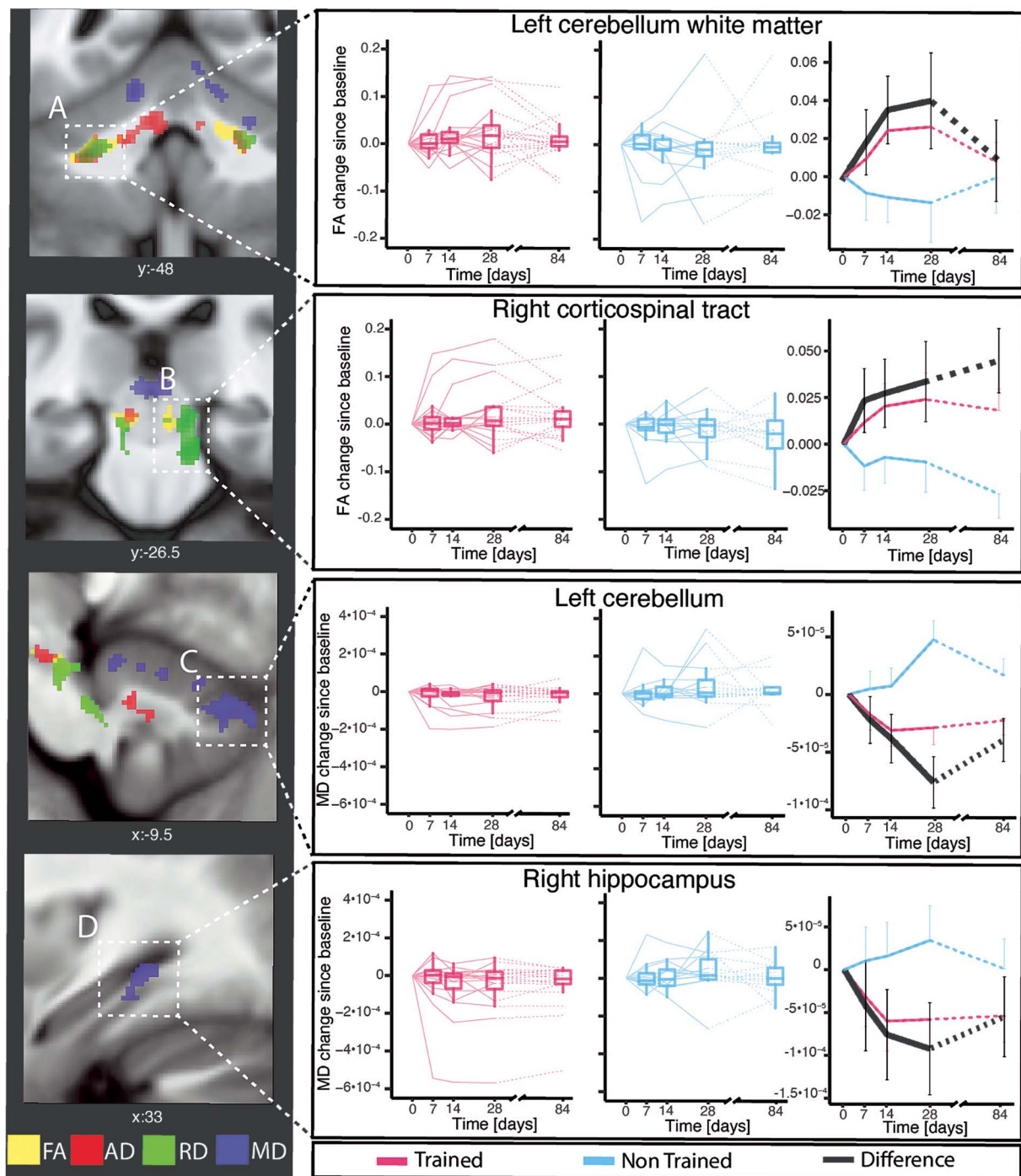
Fig. 2. Selection of training-induced changes observed during the learning of the motor skill task (combined upper and lower limb in magenta), compared to untrained healthy controls (cyan). Positive linear fractional anisotropy (FA in yellow) changes were observed in the (A) cerebellum and (B) corticospinal tract. Negative linear mean diffusivity (MD in blue) changes were observed in the (C) cerebellum and (D) hippocampus. Axial diffusivity (AD) is shown in red and radial diffusivity (RD) is shown in green. Significant clusters are overlaid on the group mean MT$_{sat}$ map for visual purposes. Slight misalignment due to potentially imperfect coregistration of the DTI-derived maps and qMRI and/or the anatomical atlases is possible. The black line indicates the differences between trained and untrained subjects (trained − untrained). The dashed lines represent the period without any training.

and faster RT improvement (FA: $z = 3.919$, $P = 0.029$; AD: $z = 4.870$, $P = 0.016$, Supplementary Table 3 and Supplementary Fig. 3).

ROI-based analysis

At baseline, faster RT was found to have a negative correlation with baseline AD values in the left cerebellum (Cluster 1: $z = 4.746$, $P = 0.013$; Cluster 2: $z = 4.182$, $P = 0.038$; Table 2 and Fig. 3) and

with baseline FA values in the left corticospinal tract ($z = 3.528$, $P = 0.022$).

Somatotopic effects of lower versus upper limb training

Within the lower limb subregion of the right corticospinal tract, lower-limb trainees exhibited a steeper linear decrease in RD

Table 2. Correlations at baseline between fractional anisotropy (FA), axial diffusivity (AD), and response time (RT). R = right, L = left.

ROI	MAP	Contrast	P-value (FWE-corrected)	Cluster size	z-value	x (mm)	y (mm)	z (mm)
Cerebellum WM L	AD	A negative association between AD and RT at baseline	0.013	96	4.746	−21	−49.5	−34.5
Cerebellum WM L	AD	A negative association between AD and RT at baseline	0.038	65	4.182	−7.5	−54	−25.5
Corticospinal tract WM L	FA	A negative association between FA and RT at baseline	0.022	79	3.528	−18	−6	−3
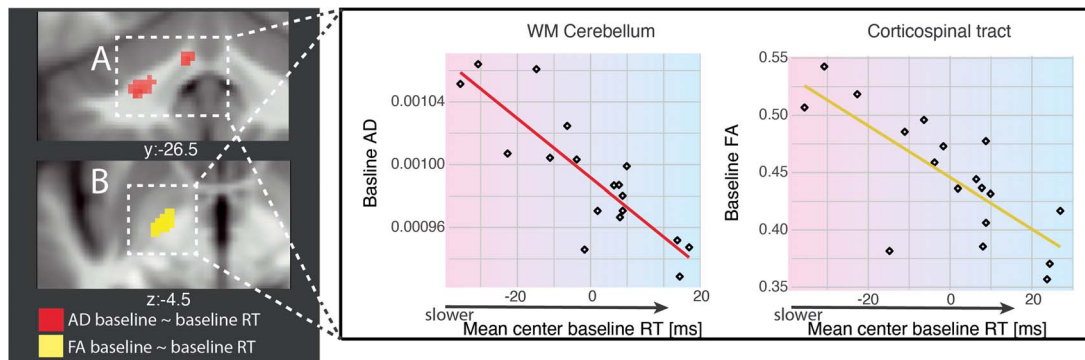
Fig. 3. Associations between baseline (A) axial diffusivity (AD) and (B) fractional anisotropy (FA) and baseline response time (RT, centered mean). Significant clusters are overlaid on the group mean MT_{sat} map for visual purposes. Slight misalignment due to potentially imperfect coregistration of the DTI-derived maps and qMRI and/or the anatomical atlases is possible. The scatter graphs depict the model average within the significant cluster with a baseline value and an approximation of the linear change for individual subjects.

Table 3. Longitudinal statistical parametric mapping (SPM) analysis showing differences in the linear and quadratic time dependence for fractional anisotropy (FA), axial diffusivity (AD), radial diffusivity (RD), and mean diffusivity (MD) between upper limb trainees and lower limb trainees. R = right, L = left.

ROI	MAP	Contrast	P-value (FWE-corrected)	Cluster size	z-value	x (mm)	y (mm)	z (mm)
Corticospinal tract WM R	FA	lin upper < lower limb	0.018	65	4.450	9	−33	−21
Corticospinal tract WM R	RD	lin upper > lower limb	<0.001	399	4.969	12	−28.5	−12
Cerebellum GM L	MD	quad upper < lower limb	0.022	105	4.378	−42	−73.5	−48

(right: z = 4.969, P < 0.001; Fig. 4A and Table 3) and steeper linear increase in FA (z = 4.450, P = 0.018; Fig. 4A and Table 3) compared to upper limb trainees. Furthermore, in the left cerebellum, upper limb trainees demonstrated larger negative quadratic changes (i.e. initial decreases) in MD (z = 4.378, P = 0.022; Fig. 4B and Table 3) within the upper limb subregion of the cerebellum, compared to lower-limb trainees.

Persistence of microstructural changes

When investigating the significant clusters extracted from the whole-brain and ROI approach, only the significant RD changes in the corona radiata near the left motor cortex and the significant MD changes in the left caudate showed differences between trainee and non-trainee subjects at day 84 in the whole-brain approach [trainees vs. non-trainees; RD: $(0.54 \pm 0.04) \bullet 10^{-3}$ mm²/s vs. $(0.58 \pm 0.03) \bullet 10^{-3}$ mm²/s, P = 0.005; MD: $(0.81 \pm 0.08) \bullet 10^{-3}$ mm²/s vs. $(0.87 \pm 0.06) \bullet 10^{-3}$ mm²/s, P = 0.049, Supplementary Table 2]. The Bayes factor in favor of H_0 over H_1 (BF_{01}) showed that H_0 was mostly favored, with weak to no evidence supporting the H_1 hypothesis in a few cases ($0.31 < BF_{01} < 1$). The Bayes factor is the likelihood ratio of the null hypothesis relative to the alternative hypothesis

(i.e. a Bayes factor of 0.05 means that the null hypothesis is 20 times less likely than the alternative). The exception was change in RD in the corona radiata near the left motor cortex, where substantial evidence ($BF_{01} = 0.133$) suggests that the trained group still has lower RD compared to the non-trained group at day 84 (Supplementary Table 2). No evidence against the H_0 hypothesis was found in the trained group between 28 and 84 days, although evidence *for* the H_0 was low, falling within the minimal to substantial range, according to Kass and Raftery (1995) ($4.1 > BF_{01} > 1$; Table 1 and Supplementary Table 2).

Coherent changes within the cranial corticospinal tract and cerebellar systems

A positive correlation was observed between the left and right corticospinal tract for FA, AD, and RD changes (Fig. 5 and Table 4). Additionally, a positive correlation was found between the left and right cerebellum for FA and MD changes (Fig. 5 and Table 4). In the time-lagged analyses, it was observed that changes in FA in the left corticospinal tract at a given timepoint were positively correlated with changes in FA in the right cerebellum at the subsequent timepoint (P < 0.001, Fig. 5 and Table 4). Furthermore, FA changes
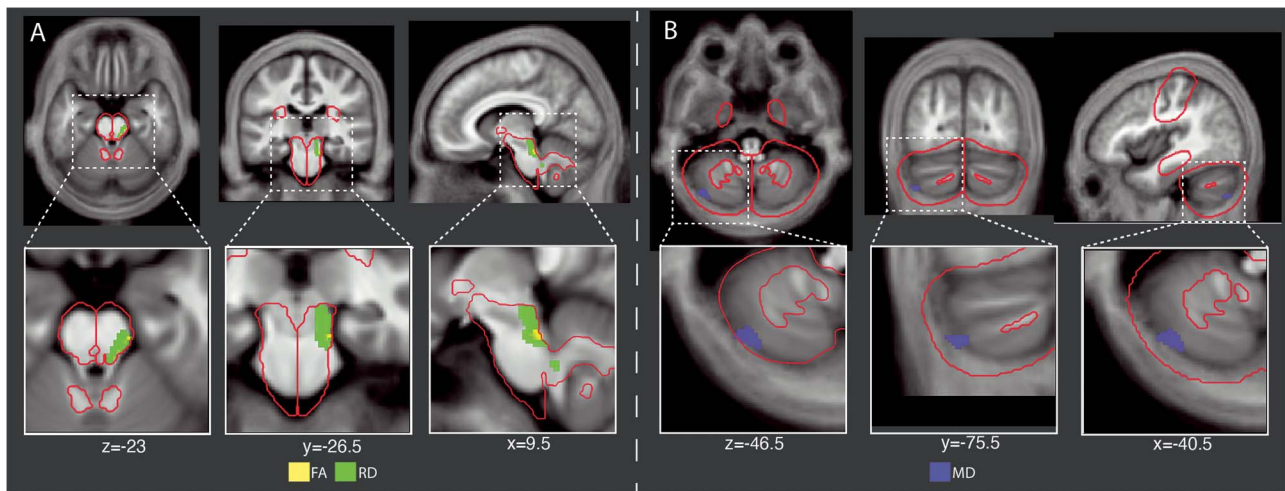
Fig. 4. Somatotopic differences associated with training the upper vs lower limbs. (A) Lower-limb training resulted in a greater linear increase in fractional anisotropy (FA in yellow) and a greater linear decrease in radial diffusivity (RD in green) in the left corticospinal tract, where the lower-limb fibers are located. (B) Training of the upper limbs resulted in a greater linear decrease in mean diffusivity (MD in blue) in the upper-limb area of the right cerebellum compared to lower-limb training. The region of interest (ROI) outline is superimposed in red. Significant clusters are overlaid on the group mean MT_{sat} map for visual purposes. Slight misalignment due to potentially imperfect coregistration of the DTI-derived maps and qMRI and/or the anatomical atlases is possible.

Table 4. Results from the in-time (i.e. no time shift in the same brain area contralateral hemisphere) and time-lag analysis (i.e. time shift in the corticospinal tract to contralateral cerebellum) for fractional anisotropy (FA), axial diffusivity (AD), radial diffusivity (RD), and mean diffusivity (MD).

Map temporal association	Coefficient	Standard error	z-value	P-value*	95% Confidence interval
In-time correlated					
Left corticospinal tract (FA) and right corticospinal tract (FA) in-time	0.907	0.064	14.26	<0.001	0.783–1.032
Left corticospinal tract (AD) and right corticospinal tract (AD) in-time	0.776	0.150	5.18	<0.001	0.482–1.070
Left corticospinal tract (RD) and right corticospinal tract (RD) in-time	0.757	0.040	19.07	<0.001	0.680–0.835
Left cerebellum (FA) and right cerebellum (FA) in-time	0.829	0.049	16.79	<0.001	0.732–0.925
Left cerebellum (MD) and right cerebellum (MD) in-time	1.020	0.049	20.88	<0.001	0.925–1.116
Correlated with a time shift of one prior timepoint					
Left corticospinal tract (FA) on the right cerebellum (FA) on the following timepoint	0.598	0.110	4.37	<0.001	0.383–0.813
Right corticospinal tract (FA) on the left cerebellum (FA) on the following timepoint	0.390	0.112	3.49	0.008	0.171–0.609

in the right corticospinal tract were positively correlated with the left cerebellum at the following timepoint ($P = 0.008$, Fig. 5 and Table 4). In short, corticospinal changes predicted subsequent cerebellar changes.

Contextualizing training-induced plasticity of DTI with qMRI

Within the WM, we observed overlapping findings between MT_{sat} (as reported in Azzarito et al. 2023) and FA, AD, and RD within the intracranial corticospinal tract (Fig. 6). Specifically, trainees exhibited a positive quadratic effect (i.e. initial decrease) in MT_{sat}, a linear increase in FA and AD, and a linear decrease in RD. Outside the WM, findings also overlapped within the GM of the cerebellum, where the trained group exhibited significant linear decreases in effective transverse relaxation rate (R2*) and MD (Fig. 6).

Comparison of the DTI and qMRI changes in response to training in GM revealed that MD and R2* both showed linear decreases (Supplementary Fig. 4), while MT_{sat}, longitudinal relaxation rate (R1), and R2* exhibited a positive quadratic (i.e. initial decrease) effect. In the WM, FA and AD showed a linear increase, whereas RD

showed a decrease and MT_{sat} showed a positive quadratic change (Supplementary Fig. 4).

Discussion

This study provides further insights into the microstructural changes that occur in the brain during sensorimotor skill acquisition. We demonstrate microstructural correlates of plasticity in key brain regions involved in motor learning, including the corticospinal tract, cerebellum, hippocampal formation, and thalamus. The majority of these changes were persistent and were associated with performance improvements. Crucially, the diffusion parameters exhibited correlations with baseline performance, suggesting that the subjects' capacity to perform a specific motor task can be estimated beforehand. This hints at the neurological underpinnings, such as the degree of myelination, influencing the MRI markers used in this study. These findings suggest a sequential pattern of training-induced plasticity, with the corticospinal tract showing early responses followed by comparable changes in the cerebellum, indicating a specific trajectory of neuroplastic adaptation within the motor system
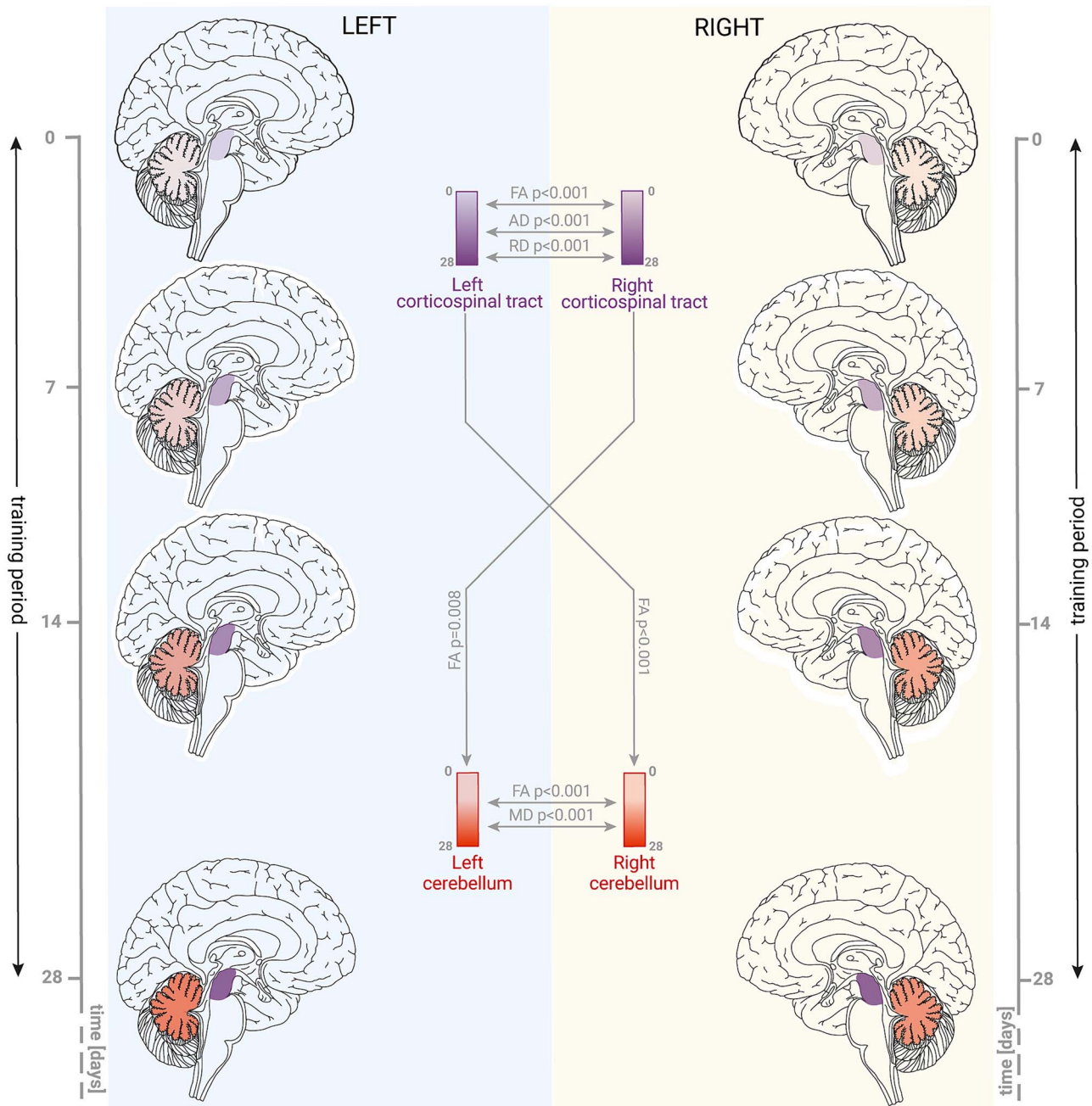
Fig. 5. Schematic representation of the coherent changes in fractional anisotropy (FA), axial diffusivity (AD), radial diffusivity (RD), and mean diffusivity (MD) between the corticospinal tract (purple) and cerebellum (red) over time during training. Single-headed arrows indicate the time-shifted analysis, indicating the temporal time lag between the two brain structures, while a double-headed arrow indicates a correlation in time between both brain areas. The gradient color changes within the boxes and the brain indicate the evolution of the convex course of linear changes observed over time.

during skill acquisition. Upper- and lower-limb trainees exhibited microstructural changes in WM (FA and RD) and GM (MD) at different locations within the corticospinal tract and cerebellum, consistent with somatotopic organization.

The training induces microstructural responses

DTI is a valuable tool for assessing microstructural changes in WM and GM (Edwards et al. 2017; Georgiadis et al. 2021). Among available DTI metrics, RD has been found to be relatively specific to the integrity of myelin (Song et al. 2002; Sun et al. 2006; Georgiadis et al. 2021), while AD has been associated with the integrity of axonal cytoarchitecture (Song et al. 2003; Budde et al.

2007; Kim et al. 2007; Sun et al. 2008; Zhang et al. 2009; Xie et al. 2011; Brennan et al. 2013). Given that FA depends on both AD and RD, it is influenced by both axonal and myelin changes (Beaulieu 2011). Within brain regions with largely isotropic diffusion patterns, such as the GM of cortical and subcortical regions, MD has been shown to be sensitive to changes in microstructure, with increases in MD observed in diseases like frontotemporal dementia, semantic dementia, progressive nonfluent aphasia, and Alzheimer's disease (Whitwell et al. 2010; Weston et al. 2015).

During 1 month of active training in StepMania, we observed progressive and tissue-specific changes in FA, RD, AD, and MD in key brain areas associated with motor skill learning, including the
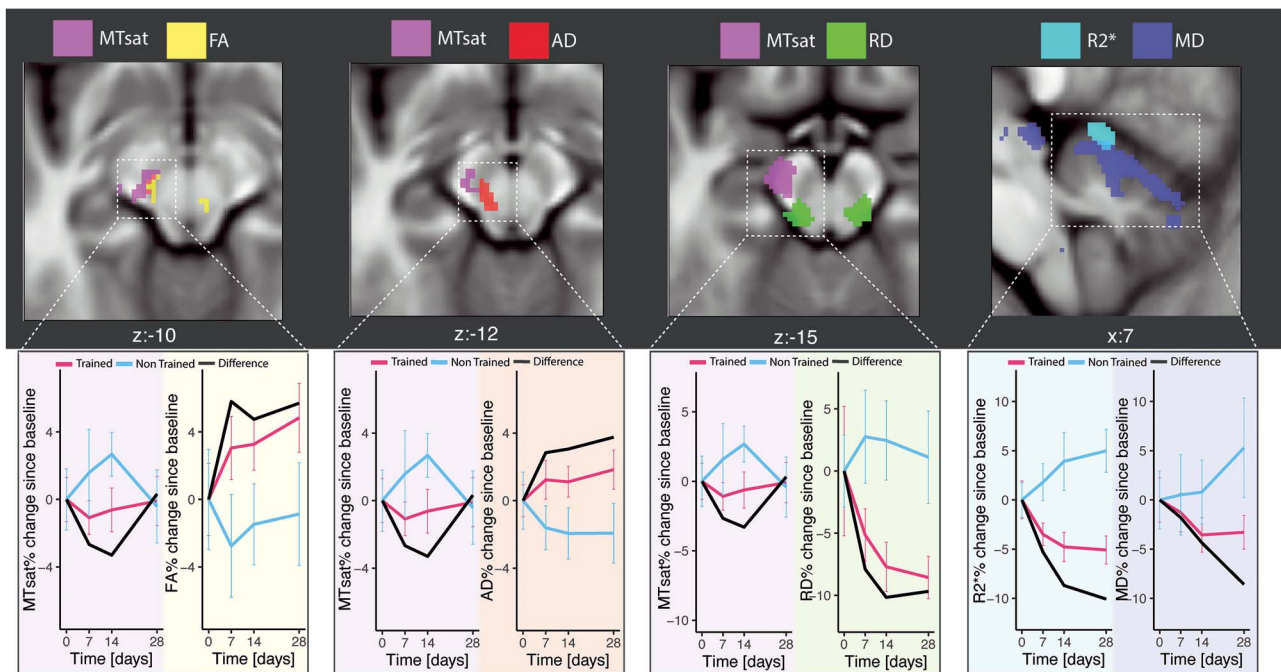
Fig. 6. Overlap between significant multiparameter mapping (MPM) changes in the study by Azzarito et al. (2023) and diffusion changes in the present study. (E) Significant group differences in fractional anisotropy (FA; yellow) and magnetization transfer saturation (MT$_{sat}$; magenta) overlapped in the corticospinal tract at the level of the crus cerebri. Significant group differences in axial diffusivity (AD; red) and MT$_{sat}$ (magenta) overlapped in the corticospinal tract at the level of the crus cerebri. Significant group differences in radial diffusivity (RD; green) and MT$_{sat}$ (magenta) overlapped in the corticospinal tract at the level of the crus cerebri. Significant group differences in mean diffusivity (MD; blue) and effective transverse relaxation rate (R2∗; cyan) overlapped in the gray matter of the cerebellum. The overlapping clusters between MPM and diffusion measures indicate regions where both modalities showed significant group differences, suggesting potential associations between microstructural changes captured by MPM and diffusion protocols; significant clusters are overlaid on the group mean MT$_{sat}$ map for visual purposes. Slight misalignment due to potentially imperfect coregistration of the DTI-derived maps and qMRI and/or the anatomical atlases is possible.

corticospinal tract, cerebellum, and hippocampal systems. Most of these microstructural markers increased during the training period, peaking at day 28, with apparent deceleration thereafter (Fig. 2). By day 84, 2 months after any training, the diffusion parameters appeared to have returned to baseline, as no significant differences were found compared to the non-trained group. In rodents, using MRI and immunohistology, it has been shown that an asymptotic or quadratic time course is a much more typical response to training than linear changes (Mediavilla et al. 2022).

The corticospinal tract, which transmits signals from the motor cortex to the motoneuron pool in the spinal cord's anterior horns, exhibited bilateral increases in FA and AD, and a decrease in RD, in response to training, suggesting increased myelination and/or fiber density (Zatorre et al. 2012; Sampaio-Baptista and Johansen-Berg 2017). Interestingly, the observed training-induced plasticity in the corticospinal tract overlapped with the transient changes in myelin-sensitive MT$_{sat}$ previously observed (Azzarito et al. 2023), suggestive of axonal reorganization followed by or concurrent with myelin plasticity (Fig. 6). Alternatively, in the study by Mediavilla et al. (2022), such findings are interpreted as myelin changes, particularly due to changes in length density (calculated as the length of myelinated fibers per unit tissue volume) of the myelinated axons. These changes can be influenced by the remodeling of existing myelin sheaths and the addition of new myelin onto previously unmyelinated regions of axons, either by newly recruited or pre-existing oligodendrocytes. In the cerebellum, we observed bilateral training-induced linear increases in FA and AD, and a decrease in RD (extending into the corticospinal tract) within the WM, as well as bilateral linear decreases in MD

within the GM. A linear decrease in MD was also seen within the GM of the bilateral thalamus and right hippocampal formation. The decrease in MD may be the result of increased axonal, dendritic, and/or myelin content and potentially attributed to processes such as synaptogenesis, angiogenesis, gliogenesis, or myelin remodeling (Adams et al. 1997; Kleim et al. 2002; Ruegg et al. 2003; Dong and Greenough 2004; Pereira et al. 2007; Canu et al. 2009; Yang et al. 2009; Toscano-Silva et al. 2010; Tronel et al. 2010; Rhyu et al. 2010; Blumenfeld et al. 2011; Yasuda et al. 2011; Zatorre et al. 2012; Sampaio-Baptista et al. 2013, 2020; Fields 2015; Sampaio-Baptista and Johansen-Berg 2017). The decrease in MD within the cerebellum overlapped with the linear decreases in R2∗ reported by Azzarito et al. (2023) (Fig. 6), indicative of processes that consume iron, such as synaptic sprouting and dendritic branching (Carlson et al. 2007; Tran et al. 2015).

Associations with performance improvements

Subjects with higher baseline FA and AD showed better task performance at baseline (Fig. 3), indicating that the state of connectivity of neuronal circuits within an individual may influence learning efficacy for a specific motor task beforehand. Moreover, the linear changes in FA and AD in the corticospinal tract at the level of the corona radiata were associated with improvement in RT (Supplementary Fig. 3). The abundant projections between the lateral cerebellum and sensorimotor cortical regions underline its role in various aspects of motor control, including visuospatial cognition (Burciu et al. 2013; Brissenden et al. 2018) and the anticipatory postural adjustments required for mastering StepMania.

Somatotopic effects of lower versus upper limb training

Somatotopic effects analysis, within the corticospinal tract, revealed differences in the magnitude of microstructural changes between upper- and lower-limb trainees (Fig. 4). The spatial pattern of these differences is consistent with the somatotopic anatomy of the corticospinal tract, where upper-limb fibers are located ventrally and lower-limb fibers more dorsally (Lemon and Morecraft 2023). The observed spatial pattern of imaging findings suggests a somatotopic representation only above the pyramidal tracts, but not within or below them, which aligns with the findings of Lemon and Morecraft (2023). Also, within the cerebellum, crucial for motor function optimization, training-specific MD changes may be evidence of focal adaptation of the specific task trained (Boillat et al. 2020).

Coherent changes within the cranial corticospinal tract and cerebellar systems

Acquiring five longitudinal scans allowed us to explore temporal associations between microstructural changes across subcortical and cortical areas involved in the motor learning task. Our analysis revealed three key interdependencies. Firstly, we observed a correlation between progressive changes in the left and right hemispheres at a given timepoint, which is expected in a bimanual/bipedal task and consistent with the bilateral MT_{sat} changes reported in Azzarito et al. (2023). Secondly, we found that progressive increases in FA in the left corticospinal tracts were associated with subsequent progressive increases in FA in the right cerebellum. Similarly, progressive increases in FA in the right corticospinal tracts were linked to later progressive increases in FA in the left cerebellum. These findings suggest that the corticospinal tract undergoes training-related changes first, followed by the cerebellum, which fine-tunes and optimizes motor learning. The delay in neuroplastic responses might point to a hierarchical rather than a parallel system (Macpherson et al. 2021). Regarding rehabilitation training in various neurological conditions, it would be interesting to investigate whether such a time-lag pattern is altered or if neuroplastic responses might not occur because the antecedent system in the hierarchy cannot adapt to the new task.

Neurobiology underpinning MRI outcomes related to training

The mechanisms underlying motor learning in humans are complex and subject to ongoing research. Key factors believed to contribute to these processes include synaptogenesis, angiogenesis, gliogenesis, and modifications in myelin such as changes in thickness, internode length, and nodes of Ranvier (Adams et al. 1997; Kleim et al. 2002; Ruegg et al. 2003; Dong and Greenough 2004; Pereira et al. 2007; Fields 2008, 2011, 2015; Canu et al. 2009; Yang et al. 2009; Toscano-Silva et al. 2010; Tronel et al. 2010; Rhyu et al. 2010; Blumenfeld et al. 2011; Yasuda et al. 2011; Zatorre et al. 2012; Sampaio-Baptista et al. 2013, 2020; Sampaio-Baptista and Johansen-Berg 2017). Studies in murine models have linked structural changes in the visual, somatosensory, and motor cortices with performance improvements, suggesting a role for oligodendrogenesis and myelination in these processes (Lamprecht and LeDoux 2004; Theodosis et al. 2008; Gibson et al. 2014; Badea et al. 2019). During synaptogenesis in the GM, a decrease in MD may occur due to increased synaptic density. This phase is followed by synaptic pruning (Kantor and Kolodkin 2003; Yasuda et al. 2011), where redundant connections

are removed, and new connections undergo activity-dependent myelination (Fields 2015; Sampaio-Baptista and Johansen-Berg 2017). These parallel mechanisms of pruning and activity-dependent myelination can influence MD, which may explain the less prominent MD changes observed between days 14 and 28. However, synaptogenesis is unlikely to play a significant role in WM tracts, where we observed similar effects in FA, AD, and RD.

Myelin remodeling, with or without significant synaptogenesis, may also explain the observed trajectories in WM. Linear changes in RD and FA in the bilateral corticospinal tract suggest myelin changes, while additional increases in AD and FA can be found in the cerebellum. Observations of oligodendrogenesis, the generation of oligodendrocyte precursor cells responsible for myelination, in trained rodents (Gibson et al. 2014) and the association of impaired motor learning with inhibited oligodendrogenesis (McKenzie et al. 2014) reinforce the role of mature oligodendrocytes in adult humans, who exhibit a stable oligodendrocyte population with low turnover rates (Yeung et al. 2014; Bacmeister et al. 2022). Recent findings in adult mice also suggest a staged response to motor training, with retraction of pre-existing myelin sheaths followed by new myelination during the consolidation of learning (Bacmeister et al. 2022). While our observations align with the trajectories in myelin-sensitive MR parameters, further mechanistic studies are necessary to determine the extent to which our findings reflect underlying neural and/or myelination processes.

Progressive changes in FA, MD, AD, and RD may, alternatively, reflect increased microstructural complexity due to training-induced gliogenesis (Fields 2015; Badea et al. 2019). This is consistent with early research indicating local tissue volume expansion in response to training (Draganski and May 2008; Zatorre et al. 2012). Observations of transient increases in vascular volume due to physical exercise (Rhyu et al. 2010) are not consistently supported by human neuroimaging studies analyzing cerebral blood volume (Thomas et al. 2016). This study did not provide evidence for such mechanistic changes, as FA decrease, and AD and RD increases would be expected rather an FA and AD increase and RD decrease. Given that both angiogenesis and gliogenesis involve changes in non-neural substrates common to both GM and WM, it is possible that either or both of these processes co-occur during the aforementioned training processes.

Contextualizing training-induced plasticity of DTI metrics with MPM findings

Our findings revealed training-induced plasticity in diffusion parameters in parallel to plasticity as measured by MT_{sat}, R1, and R2∗. The concurrent observation of changes in diffusion parameters and other quantitative MRI parameters have also been reported for other biological processes such as aging (Draganski et al. 2011). Combining multiple MRI parameters sensitive to different biological aspects sheds light, non-invasively, on the underlying biological processes during human motor task learning. Substantial spatial overlap between MT_{sat} and FA, AD, RD, as well as between R2∗ and MD was observed. One of many potential explanations of the positive quadratic MT_{sat} changes is synaptic and dendritic branching, which might initially lead to a relative MT_{sat} decrease due to the lowered myelin concentration caused by newly formed dendrites and axons. Subsequently, myelination of the newly formed axons and/or pruning of non-essential connections occurs, increasing the relative myelin content.

The addition of corroborative DTI measures allows for refinement of this hypothesis and highlights the complementary of

these approaches. We observed linear FA and AD increases and RD decreases overlapping with transient MPM changes (Fig. 6). This overlap supports the theory of an increase in axon density in response to training which is followed by a later, consolidatory increase in myelinization. In the GM, conversely, parallel linear decreases in MD and R2∗ were observed. These findings support the hypothesis of dendritic sprouting and axonal branching, both processes in which iron consumption occurs (Carlson et al. 2007; Tran et al. 2015), decreasing the R2∗ signal and increasing microstructural density, leading to a decrease in MD (Whitwell et al. 2010; Draganski et al. 2011). There was also spatial overlap of FA and MT_sat in the study conducted by Draganski et al. (2011), which assessed qMRI and DTI parameters and their association with aging. However, they did not demonstrate any overlap between MD and R2∗ in their heterogeneous cohort, in which age ranged from 18 to 85 years in contrast to the current study (23 to 62 years). The absence of such an overlap might be due to their study's lack of a longitudinal design. Alternatively, the processes of aging might influence qMRI and DTI parameters differently than training, leading to a disparity in the changes observed in MD and R2∗. In diseases such as Huntington's disease, where neuron loss and gliosis are combined with accumulations of iron, there is an inverse relationship between MD and T2 (Syka et al. 2015), which might be less pronounced in the aging process alone.

MPM and DTI parameters also offer specific insights beyond these overlapping regions, evidenced by the fact that not all clusters capturing change overlapped. This distinctiveness can be attributed to their entirely different physics which result in differential sensitivities and specificities to underlying microstructure. dMRI relies on diffusion barriers, while qMRI based on relaxometry, such as the MPM protocol, is sensitive to macromolecular content (Does 2018; Natu et al. 2019; Novikov et al. 2019; Weiskopf et al. 2021). Therefore, combining independent imaging methodologies might allow the investigation of the same underlying biological mechanisms with different sensitivity and specificity to different aspects of this process. This addresses the limitation of current MRI methods, which cannot capture processes comprehensively with a single measure (van Weijden et al. 2021). In the case of myelin, it has been shown that R1, MT_sat, and RD are sensitive to myelin content, though they are based on different physical principles. In brief, R1 is based on the single exponential spin–lattice relaxation, which varies with tissue composition, while MT_sat quantifies the magnetization transfer from macromolecules, predominantly myelin, to free water, and RD measures water diffusion perpendicular to the main diffusion direction along the axons (van der Weijden et al. 2023). Furthermore, the typical resolution for dMRI (ca. 2 to 3 mm isotropic) is lower than that for qMRI (ca. 1 mm isotropic), leading to more severe partial volume effects, potentially contributing to the lower sensitivity of dMRI within cortical GM structures. Adopting a multicontrast MRI approach increases the capacity to detect biological processes, particularly when both qMRI and dMRI indicate neuroplasticity. This approach enhances the likelihood of distinguishing neuroplasticity changes from non-systematic signal fluctuations that might not be detected by one method alone.

Limitations

This study has some shortcomings that should be taken into account. A significant difference in %CSR at baseline between the upper- and lower-limb trainees (higher for upper limb trainees) was detected, which could potentially decrease the %CSR improvements of the upper limb trainees. To address this,

exponential models were chosen to incorporate a plateauing effect, and nonparametric tests were used to account for the nonnormal distribution that may result. Only one subject achieved a perfect %CSR score during the training period. Due to differences in the degree of improvement in %CSR, additional somatotopic representation differences may have gone undetected.

The DTI metrics including FA, MD, AD, and RD are sensitive, but not specific, measures of WM and GM microstructure, serving as proxies in the absence of confirmatory histological training studies. Nevertheless, we demonstrated coherent changes consistent with the current understanding of the processes underpinning complex motor learning tasks (Lungu et al. 2014), with several spatial overlaps identified with independent microstructural markers for myelin observed in the same training cohort (MT_sat and R1 and iron deposition R2∗; Azzarito et al. 2023).

The resolution and smoothing used in this study may lead to partial volume effects and therefore decreased accuracy in distinguishing individual fiber tracts. We have attempted to minimize the impact of this on the quantitative metrics by using tissue-specific smoothing (Draganski et al. 2011). The potential remaining partial volume effects and other sources of noise could potentially explain the absence of upper- and lower-limb changes in GM and WM regions in close proximity, as well as potential influences from neighboring brain areas or fiber tracts.

Analyses in this study were limited to linear and quadratic temporal changes, although clearly other temporal patterns are possible. The quadratic model is particularly suitable for the detection of progressive changes and transient changes such as expansion and renormalization processes in the brain during learning (Draganski et al. 2006; Moraud et al. 2016; Hopkins et al. 2018). Furthermore, only healthy young to middle-aged males were investigated to avoid potential influences of sex on neuroplastic changes, which might differ in temporal, spatial, or magnitude aspects. This limitation may affect the generalizability to cohorts that include females. Nevertheless, since the majority of patients with incomplete spinal cord injury, the therapeutic target of the training intervention under investigation, are young to middle-aged males (Jackson et al. 2004), this study can provide valuable knowledge for most patients.

For some DTI metrics, we observed longitudinal fluctuations in the untrained group. From GM morphometry studies (Langer et al. 2012; Streitbürger et al. 2012; Campabadal et al. 2021), it is already known that factors such as hydration, sleep, or head positioning as well as scan–rescan variability might influence local GM changes in plasticity studies and may have played a role in this study. For example, patients with sleep disorders have reduced GM in various brain regions, including the hippocampal formation, compared to normal sleepers (Campabadal et al. 2021). Dehydration may also cause GM volume decreases (Streitbürger et al. 2012). In this study, scans were acquired on weekdays at similar timepoints and never after training. Furthermore, the nontrained group was instructed not to acquire any new skills, e.g. not to take dance lessons, during the course of the study but to continue with their previous daily habits. The requirement to attend scans may have resulted in disruption or a reduction in overall daily activity that was not controlled for in the training groups, and this could potentially lead to structural brain changes such as FA and cortical thickness changes (Langer et al. 2012). However, given that group assignment was pseudorandomized, the significant group trajectory differences (i.e. the interaction between group and time) can be attributed to the effects of motor training (Fig. 2). This is particularly evident as no systematic differences over time in registration quality or in the residual

sum-squared error of the tensor fitting were found between the trained group and the non-trained group (Supplementary Table 4). Nevertheless, the temporal drift due to the factors mentioned above might have affected both groups similarly. This would cause additional variability in the data and could bias the observed group differences.

Conclusion

Longitudinal DTI, sensitive to the integrity and geometry of axonal fibers, revealed changes across the corticospinal, cerebellar, thalamic, and hippocampal systems in individuals mastering the motion game StepMania. These changes followed a systematic and progressive time course, consistent with increasing myelination and/or changes in the tissue composition, e.g. reduction of the extra-axonal space due to increased fiber or astrocyte density. In the corticospinal tract and cerebellum of upper- and lower-limb trainees, somatotopic differences in the magnitude of changes were observed, providing further evidence of a somatotopy of motor skill learning. By correlating microstructural changes across regions and timepoints, we revealed a coherent and choreographed motor learning network, encompassing the corticospinal tract and the cerebellum. These results provide further insights into the coordinated plasticity of a corticospinal-cerebellar network, which underlies skill acquisition in the healthy human brain. Through non-invasive MRI techniques, we contribute to the enhanced understanding and measurement of the neural plasticity that underpins skill acquisition, offering valuable insights for future research and clinical applications.

Acknowledgments

Author contributions

Tim Emmenegger (Conceptualization, Formal analysis, Investigation, Methodology, Validation, Visualization, Writing—original draft), Gergely David (Conceptualization, Formal analysis, Methodology, Writing—review & editing), Siawoosh Mohammadi (Conceptualization, Data curation, Investigation, Methodology, Writing—review & editing), Gabriel Ziegler (Investigation, Methodology, Supervision, Writing—review & editing), Martina Callaghan (Conceptualization, Investigation, Methodology, Supervision), Alan Thompson (Conceptualization, Methodology, Supervision, Writing—review & editing), Karl Friston (Conceptualization, Methodology, Supervision, Writing—review & editing), Nikolaus Weiskopf (Conceptualization, Investigation, Methodology, Supervision, Writing—review & editing), Tim Killeen (Conceptualization, Formal analysis, Methodology, Project administration, Writing—review & editing), and Patrick Freund (Conceptualization, Data curation, Funding acquisition, Investigation, Methodology, Project administration, Supervision, Writing—review & editing).

Funding

References

Adams B, Lee M, Fahnestock M, Racine RJ. Long-term potentiation trains induce mossy fiber sprouting. *Brain Res*. 1997:775(1–2): 193–197. https://doi.org/10.1016/S0006-8993(97)01061-5.

Ashburner J. A fast diffeomorphic image registration algorithm. *NeuroImage*. 2007:38(1):95–113. https://doi.org/10.1016/j.neuroimage.2007.07.007.

Ashburner J. Symmetric diffeomorphic modeling of longitudinal structural MRI. *Front Neurosci*. 2013:6:197. https://doi.org/10.3389/fnins.2012.00197.

Ashburner J, Friston KJ. Unified segmentation. *NeuroImage*. 2005:26(3):839–851. https://doi.org/10.1016/j.neuroimage.2005.02.018.

Azzarito M, Emmenegger TM, Ziegler G, Huber E, Grabher P, Callaghan MF, Thompson A, Friston K, Weiskopf N, Killeen T, et al. Coherent, time-shifted patterns of microstructural plasticity during motor-skill learning. *NeuroImage*. 2023:274:120128. https://doi.org/10.1016/j.neuroimage.2023.120128.

Bacmeister CM, Huang R, Osso LA, Thornton MA, Conant L, Chavez AR, Poleg-Polsky A, Hughes EG. Motor learning drives dynamic patterns of intermittent myelination on learning-activated axons. *Nat Neurosci*. 2022:25(10):1300–1313. https://doi.org/10.1038/s41593-022-01169-4.

Badea A, Ng KL, Anderson RJ, Zhang J, Miller MI, O'Brien RJ. Magnetic resonance imaging of mouse brain networks plasticity following motor learning. *PLoS One*. 2019:14(5):e0216596, 1–21. https://doi.org/10.1371/journal.pone.0216596.

Basser PJ, Mattiello J, LeBihan D. MR diffusion tensor spectroscopy and imaging. *Biophys J*. 1994:66(1):259–267. https://doi.org/10.1016/S0006-3495(94)80775-1.

Beaulieu C. What makes diffusion anisotropic in the nervous system? In: Jones DK, editors. *Diffusion MRI theory, methods, and applications*. New York: Oxford University Press; 2011. pp. 92–109.

Bengtsson SL, Nagy Z, Skare S, Forsman L, Forssberg H, Ullén F. Extensive piano practicing has regionally specific effects on white matter development. *Nat Neurosci*. 2005:8(9):1148–1150. https://doi.org/10.1038/nn1516.

Blumenfeld-Katzir T, Pasternak O, Dagan M, Assaf Y. Diffusion MRI of structural brain plasticity induced by a learning and memory task. *PLoS One*. 2011:6(6):e20678. https://doi.org/10.1371/journal.pone.0020678.

Boillat Y, Bazin P-L, van der Zwaag W. Whole-body somatotopic maps in the cerebellum revealed with 7T fMRI. *NeuroImage*. 2020:211:116624, 1–11. https://doi.org/10.1016/j.neuroimage.2020.116624.

Boyke J, Driemeyer J, Gaser C, Buchel C, May A. Training-induced brain structure changes in the elderly. *J Neurosci*. 2008:28(28):7031–7035. https://doi.org/10.1523/JNEUROSCI.0742-08.2008.

Brennan FH, Cowin GJ, Kurniawan ND, Ruitenberg MJ. Longitudinal assessment of white matter pathology in the injured mouse spinal cord through ultra-high field (16.4T) in vivo diffusion tensor imaging. *NeuroImage*. 2013:82:574–585. https://doi.org/10.1016/j.neuroimage.2013.06.019.

Brissenden JA, Tobyne SM, Osher DE, Levin EJ, Halko MA, Somers Correspondence DC. Topographic cortico-cerebellar networks revealed by visual attention and working memory. *Curr Biol*. 2018:28(21):3364–3372.e5. https://doi.org/10.1016/j.cub.2018.08.059.

Budde MD, Kim JH, Liang H-F, Schmidt RE, Russell JH, Cross AH, Song S-K. Toward accurate diagnosis of white matter pathology using diffusion tensor imaging. *Magn Reson Med*. 2007:57(4):688–695. https://doi.org/10.1002/mrm.21200.

Burciu RG, Fritsche N, Granert O, Schmitz L, Sponemann N, Konczak J, Theysohn N, Gerwig M, van Eimeren T, Timmann D. Brain changes associated with postural training in patients with cerebellar degeneration: a voxel-based morphometry study. *J Neurosci*. 2013:33(10):4594–4604. https://doi.org/10.1523/JNEUROSCI.3381-12.2013.

Campabadal A, Segura B, Junque C, Iranzo A. Structural and functional magnetic resonance imaging in isolated REM sleep behavior disorder: a systematic review of studies using neuroimaging software. *Sleep Med Rev*. 2021:59:101495, 1–13. https://doi.org/10.1016/j.smrv.2021.101495.

Canu M-H, Carnaud M, Picquet F, Goutebroze L. Activity-dependent regulation of myelin maintenance in the adult rat. *Brain Res*. 2009:1252:45–51. https://doi.org/10.1016/j.brainres.2008.10.079.

Carlson ES, Stead JDH, Neal CR, Petryk A, Georgieff MK. Perinatal iron deficiency results in altered developmental expression of genes mediating energy metabolism and neuronal morphogenesis in hippocampus. *Hippocampus*. 2007:17(8):679–691. https://doi.org/10.1002/hipo.20307.

Chen H, Lin K, Liing R, Wu C, Chen C. Kinematic measures of arm-trunk movements during unilateral and bilateral reaching predict clinically important change in perceived arm use in daily activities after intensive stroke rehabilitation. *J Neuroeng Rehabil*. 2015:12(1):84. https://doi.org/10.1186/s12984-015-0075-8.

Chen Y, Baraz J, Xuan SY, Yang X, Castoro R, Xuan Y, Roth AR, Dortch RD, Li J. Multiparametric quantitative MRI of peripheral nerves in the leg: a reliability study. *J Magn Reson Imaging*. 2024:59(2):563–574. https://doi.org/10.1002/jmri.28778.

David G, Mohammadi S, Martin AR, Cohen-Adad J, Weiskopf N, Thompson A, Freund P. Traumatic and nontraumatic spinal cord injury: pathological insights from neuroimaging. *Nat Rev Neurol*. 2019:15(12):718–731. https://doi.org/10.1038/s41582-019-0270-5.

Dayan E, Cohen LG. Neuroplasticity subserving motor skill learning. *Neuron*. 2011:72(3):443–454. https://doi.org/10.1016/j.neuron.2011.10.008.

Diedrichsen J. A spatially unbiased atlas template of the human cerebellum. *NeuroImage*. 2006:33(1):127–138. https://doi.org/10.1016/j.neuroimage.2006.05.056.

Does MD. Inferring brain tissue composition and microstructure via MR relaxometry. *NeuroImage*. 2018:182:136–148. https://doi.org/10.1016/j.neuroimage.2017.12.087.

Dong WK, Greenough WT. Plasticity of nonneuronal brain tissue: roles in developmental disorders. *Ment Retard Dev Disabil Res Rev*. 2004:10(2):85–90. https://doi.org/10.1002/mrdd.20016.

Draganski B, May A. Training-induced structural changes in the adult human brain. *Behav Brain Res*. 2008:192(1):137–142. https://doi.org/10.1016/j.bbr.2008.02.015.

Draganski B, Gaser C, Kempermann G, Kuhn HG, Winkler J, Buchel C, May A. Temporal and spatial dynamics of brain structure changes during extensive learning. *J Neurosci*. 2006:26(23):6314–6317. https://doi.org/10.1523/JNEUROSCI.4628-05.2006.

Draganski B, Ashburner J, Hutton C, Kherif F, Frackowiak RSJ, Helms G, Weiskopf N. Regional specificity of MRI contrast parameter changes in normal ageing revealed by voxel-based quantification (VBQ). *NeuroImage*. 2011:55(4):1423–1434. https://doi.org/10.1016/j.neuroimage.2011.01.052.

Edwards LJ, Pine KJ, Ellerbrock I, Weiskopf N, Mohammadi S. NODDI-DTI: estimating neurite orientation and dispersion parameters from a diffusion tensor in healthy white matter. *Front Neurosci*. 2017:11:1–15. https://doi.org/10.3389/fnins.2017.00720.

Eickhoff SB, Stephan KE, Mohlberg H, Grefkes C, Fink GR, Amunts K, Zilles K. A new SPM toolbox for combining probabilistic cytoarchitectonic maps and functional imaging data. *NeuroImage*. 2005:25(4):1325–1335. https://doi.org/10.1016/j.neuroimage.2004.12.034.

Eickhoff SB, Paus T, Caspers S, Grosbras MH, Evans AC, Zilles K, Amunts K. Assignment of functional activations to probabilistic cytoarchitectonic areas revisited. *NeuroImage*. 2007:36(3):511–521. https://doi.org/10.1016/j.neuroimage.2007.03.060.

Fields RD. White matter in learning, cognition and psychiatric disorders. *Trends Neurosci*. 2008:31(7):361–370. https://doi.org/10.1016/j.tins.2008.04.001.

Fields RD. Imaging learning: the search for a memory trace. *Neuroscientist*. 2011:17(2):185–196. https://doi.org/10.1177/1073858410383696.

Fields RD. A new mechanism of nervous system plasticity: activity-dependent myelination. *Nat Rev Neurosci*. 2015:16(12):756–767. https://doi.org/10.1038/nrn4023.

Friston K, Moran R, Seth AK. Analysing connectivity with granger causality and dynamic causal modelling. *Curr Opin Neurobiol*. 2013:23(2):172–178. https://doi.org/10.1016/j.conb.2012.11.010.

Georgiadis M, Schroeter A, Gao Z, Guizar-Sicairos M, Liebi M, Leuze C, McNab JA, Balolia A, Veraart J, Ades-Aron B, et al. Nanostructure-specific X-ray tomography reveals myelin levels, integrity and axon orientations in mouse and human nervous tissue. *Nat Commun*. 2021:12(1):2941. https://doi.org/10.1038/s41467-021-22719-7.

Gibson EM, Purger D, Mount CW, Goldstein AK, Lin GL, Wood LS, Inema I, Miller SE, Bieri G, Zuchero JB, et al. Neuronal activity promotes oligodendrogenesis and adaptive myelination in the mammalian brain. *Science*. 2014:344(6183):1252304–1252304. https://doi.org/10.1126/science.1252304.

Han Y, Yang H, Lv Y-T, Zhu C-Z, He Y, Tang H-H, Gong Q-Y, Luo Y-J, Zang Y-F, Dong Q. Gray matter density and white matter integrity in pianists' brain: a combined structural and diffusion tensor MRI study. *Neurosci Lett*. 2009:459(1):3–6. https://doi.org/10.1016/j.neulet.2008.07.056.

Hofstetter S, Tavor I, Tzur Moryosef S, Assaf Y. Short-term learning induces white matter plasticity in the fornix. *J Neurosci*. 2013:33(31):12844–12850. https://doi.org/10.1523/JNEUROSCI.4520-12.2013.

Hopkins BS, Weber KA, Cloney MB, Paliwal M, Parrish TB, Smith ZA. Tract-specific volume loss on 3T MRI in patients with cervical spondylotic myelopathy. *Spine (Phila Pa 1976)*. 2018:43(20):E1204–E1209. https://doi.org/10.1097/BRS.0000000000002667.

Hüfner K, Binetti C, Hamilton DA, Stephan T, Flanagin VL, Linn J, Labudda K, Markowitsch H, Glasauer S, Jahn K, et al. Structural and functional plasticity of the hippocampal formation in professional dancers and slackliners. *Hippocampus*. 2011:21(8):855–865. https://doi.org/10.1002/hipo.20801.

Jackson AB, Dijkers M, DeVivo MJ, Poczatek RB. A demographic profile of new traumatic spinal cord injuries: change and stability over 30 years. *Arch Phys Med Rehabil*. 2004:85(11):1740–1748. https://doi.org/10.1016/j.apmr.2004.04.035.

Jacobacci F, Armony JL, Yeffal A, Lerner G, Amaro E, Jovicich J, Doyon J, Della-Maggiore V. Rapid hippocampal plasticity supports motor sequence learning. *Proc Natl Acad Sci*. 2020:117(38):23898–23903. https://doi.org/10.1073/pnas.2009576117.

Johansen-Berg H, Della-Maggiore V, Behrens TEJ, Smith SM, Paus T. Integrity of white matter in the corpus callosum correlates with bimanual co-ordination skills. *NeuroImage*. 2007:36(Suppl 2):T16–T21. https://doi.org/10.1016/j.neuroimage.2007.03.041.

Kantor DB, Kolodkin AL. Curbing the excesses of youth. *Neuron*. 2003:38(6):849–852. https://doi.org/10.1016/S0896-6273(03)00364-7.

Kass RE, Raftery AE. Bayes factors. *J Am Stat Assoc*. 1995:90(430):773–795. https://doi.org/10.1080/01621459.1995.10476572.

Kim JH, Loy DN, Liang H-F, Trinkaus K, Schmidt RE, Song S-K. Noninvasive diffusion tensor imaging of evolving white matter pathology in a mouse model of acute spinal cord injury. *Magn Reson Med*. 2007:58(2):253–260. https://doi.org/10.1002/mrm.21316.

Kleim JA, Barbay S, Cooper NR, Hogg TM, Reidel CN, Remple MS, Nudo RJ. Motor learning-dependent synaptogenesis is localized to functionally reorganized motor cortex. *Neurobiol Learn Mem*. 2002:77(1):63–77. https://doi.org/10.1006/nlme.2000.4004.

Kodama M, Ono T, Yamashita F, Ebata H, Liu M, Kasuga S, Ushiba J. Structural gray matter changes in the hippocampus and the primary motor cortex on an-hour-to-one-day scale can predict arm-reaching performance improvement. *Front Hum Neurosci*. 2018:12:209. https://doi.org/10.3389/fnhum.2018.00209.

La Terra D, Bjerre A-S, Rosier M, Masuda R, Ryan TJ, Palmer LM. The role of higher-order thalamus during learning and correct performance in goal-directed behavior. *elife*. 2022:11:1–21. https://doi.org/10.7554/eLife.77177.

Lakhani B, Borich MR, Jackson JN, Wadden KP, Peters S, Villamayor A, MacKay AL, Vavasour IM, Rauscher A, Boyd LA. Motor skill acquisition promotes human brain myelin plasticity. *Neural Plast*. 2016:2016:1–7. https://doi.org/10.1155/2016/7526135.

Lamprecht R, LeDoux J. Structural plasticity and memory. *Nat Rev Neurosci*. 2004:5(1):45–54. https://doi.org/10.1038/nrn1301.

Langer N, Hänggi J, Müller NA, Simmen HP, Jäncke L. Effects of limb immobilization on brain plasticity. *Neurology*. 2012:78(3):182–188. https://doi.org/10.1212/WNL.0b013e31823fcd9c.

Lemon RN, Morecraft RJ. The evidence against somatotopic organization of function in the primate corticospinal tract. *Brain*. 2023:146(5):1791–1803. https://doi.org/10.1093/brain/awac496.

Leutgeb S, Leutgeb JK, Moser M-B, Moser EI. Place cells, spatial maps and the population code for memory. *Curr Opin Neurobiol*. 2005:15(6):738–746. https://doi.org/10.1016/j.conb.2005.10.002.

Long J, Feng Y, Liao H, Zhou Q, Urbin MA. Motor sequence learning is associated with hippocampal subfield volume in humans with medial temporal lobe epilepsy. *Front Hum Neurosci*. 2018:12:1–9. https://doi.org/10.3389/fnhum.2018.00367.

Lum PS, Mulroy S, Amdur RL, Requejo P, Prilutsky BI, Dromerick AW. Gains in upper extremity function after stroke via recovery or compensation: potential differential effects on amount of real-world limb use. *Top Stroke Rehabil*. 2009:16(4):237–253. https://doi.org/10.1310/tsr1604-237.

Lungu O, Monchi O, Albouy G, Jubault T, Ballarin E, Burnod Y, Doyon J. Striatal and hippocampal involvement in motor sequence chunking depends on the learning strategy. *PLoS One*. 2014:9(8):e103885, 1–17. https://doi.org/10.1371/journal.pone.0103885.

Macpherson T, Matsumoto M, Gomi H, Morimoto J, Uchibe E, Hikida T. Parallel and hierarchical neural mechanisms for adaptive and predictive behavioral control. *Neural Netw*. 2021:144:507–521. https://doi.org/10.1016/j.neunet.2021.09.009.

Manto M, Bower JM, Conforto AB, Delgado-García JM, da Guarda SNF, Gerwig M, Habas C, Hagura N, Ivry RB, Mariën P, et al. Cerebellar function and cognition. *Pmc*. 2015:11:457–487.

Martin AR, Aleksanderek I, Cohen-Adad J, Tarmohamed Z, Tetreault L, Smith N, Cadotte DW, Crawley A, Ginsberg H, Mikulis DJ, et al. Translating state-of-the-art spinal cord MRI techniques to clinical use: a systematic review of clinical studies utilizing DTI, MT, MWF, MRS, and fMRI. *Neuroimage Clin*. 2016:10:192–238. https://doi.org/10.1016/j.nicl.2015.11.019.

Mayo NE, Wood-Dauphinee S, Côté R, Durcan L, Carlton J. Activity, participation, and quality of life 6 months poststroke. *Arch Phys Med Rehabil*. 2002:83(8):1035–1042. https://doi.org/10.1053/apmr.2002.33984.

McKenzie IA, Ohayon D, Li H, de Faria JP, Emery B, Tohyama K, Richardson WD. Motor skill learning requires active central myelination. *Science*. 2014:346(6207):318–322. https://doi.org/10.1126/science.1254960.

Mediavilla T, Özalay Ö, Estévez-Silva HM, Frias B, Orädd G, Sultan FR, Brozzoli C, Garzón B, Lövdén M, Marcellino DJ. Learning-related contraction of gray matter in rodent sensorimotor cortex is associated with adaptive myelination. *elife*. 2022:11:1–27. https://doi.org/10.7554/eLife.77432.

Moraud EM, Capogrosso M, Formento E, Wenger N, DiGiovanna J, Courtine G, Micera S. Mechanisms underlying the neuromodulation of spinal circuits for correcting gait and balance deficits after spinal cord injury. *Neuron*. 2016:89(4):814–828. https://doi.org/10.1016/j.neuron.2016.01.009.

Natu VS, Gomez J, Barnett M, Jeska B, Kirilina E, Jaeger C, Zhen Z, Cox S, Weiner KS, Weiskopf N, et al. Apparent thinning of human visual cortex during childhood is associated with myelination. *Proc Natl Acad Sci USA*. 2019:116(41):20750–20759. https://doi.org/10.1073/pnas.1904931116.

Novikov DS, Fieremans E, Jespersen SN, Kiselev VG. Quantifying brain microstructure with diffusion MRI: theory and parameter estimation. *NMR Biomed*. 2019:32(4):139–148. https://doi.org/10.1002/nbm.3998.

Orrell AJ, Eves FF, Masters RSW. Implicit motor learning of a balancing task. *Gait Posture*. 2006:23(1):9–16. https://doi.org/10.1016/j.gaitpost.2004.11.010.

Patterson TS, Bishop MD, McGuirk TE, Sethi A, Richards LG. Reliability of upper extremity kinematics while performing different tasks in individuals with stroke. *J Mot Behav*. 2011:43(2):121–130. https://doi.org/10.1080/00222895.2010.548422.

Pereira AC, Huddleston DE, Brickman AM, Sosunov AA, Hen R, McKhann GM, Sloan R, Gage FH, Brown TR, Small SA. An in vivo correlate of exercise-induced neurogenesis in the adult dentate gyrus. *Proc Natl Acad Sci*. 2007:104(13):5638–5643. https://doi.org/10.1073/pnas.0611721104.

Pi Y-L, Wu X-H, Wang F-J, Liu K, Wu Y, Zhu H, Zhang J. Motor skill learning induces brain network plasticity: a diffusion-tensor imaging study. *PLoS One*. 2019:14(2):e0210015, 1–17. https://doi.org/10.1371/journal.pone.0210015.

Prahm C, Kayali F, Sturma A, Aszmann O. *Recommendations for games to increase patient motivation during upper limb amputee rehabilitation*. Cham: Springer; 2017 pp. 1157–1161.

Prevosto V, Sommer MA. Cognitive control of movement via the cerebellar-recipient thalamus. *Front Syst Neurosci*. 2013:7:1–8. https://doi.org/10.3389/fnsys.2013.00056.

Reid LB, Sale MV, Cunnington R, Mattingley JB, Rose SE. Brain changes following four weeks of unimanual motor training: evidence from fMRI-guided diffusion MRI tractography. *Hum Brain Mapp*. 2017:38(9):4302–4312. https://doi.org/10.1002/hbm.23514.

Rhyu IJ, Bytheway JA, Kohler SJ, Lange H, Lee KJ, Boklewski J, McCormick K, Williams NI, Stanton GB, Greenough WT, et al. Effects of aerobic exercise training on cognitive function and cortical vascularity in monkeys. *Neuroscience*. 2010:167(4):1239–1248. https://doi.org/10.1016/j.neuroscience.2010.03.003.

Roby-Brami A, Feydy A, Combeaud M, Biryukova EV, Bussel B, Levin MF. Motor compensation and recovery for reaching in stroke patients. *Acta Neurol Scand*. 2003:107(5):369–381. https://doi.org/10.1034/j.1600-0404.2003.00021.x.

Ruegg DG, Kakebeeke TH, Gabriel J-P, Bennefeld M. Conduction velocity of nerve and muscle fiber action potentials after a space mission or a bed rest. *Clin Neurophysiol*. 2003:114(1):86–93. https://doi.org/10.1016/S1388-2457(02)00329-2.

Sampaio-Baptista C, Johansen-Berg H. White matter plasticity in the adult brain. *Neuron*. 2017:96(6):1239–1251. https://doi.org/10.1016/j.neuron.2017.11.026.

Sampaio-Baptista C, Khrapitchev AA, Foxley S, Schlagheck T, Scholz J, Jbabdi S, DeLuca GC, Miller KL, Taylor A, Thomas N, et al. Motor skill learning induces changes in white matter microstructure and myelination. *J Neurosci*. 2013:33(50):19499–19503. https://doi.org/10.1523/JNEUROSCI.3048-13.2013.

Sampaio-Baptista C, Vallès A, Khrapitchev AA, Akkermans G, Winkler AM, Foxley S, Sibson NR, Roberts M, Miller K, Diamond ME, et al. White matter structure and myelin-related gene expression alterations with experience in adult rats. *Prog Neurobiol*. 2020:187:101770. https://doi.org/10.1016/j.pneurobio.2020.101770.

Schlegel AA, Rudelson JJ, Tse PU. White matter structure changes as adults learn a second language. *J Cogn Neurosci*. 2012:24(8):1664–1670. https://doi.org/10.1162/jocn_a_00240.

Scholz J, Klein MC, Behrens TEJ, Johansen-Berg H. Training induces changes in white-matter architecture. *Nat Neurosci*. 2009:12(11):1370–1371. https://doi.org/10.1038/nn.2412.

Seiler A, Nöth U, Hok P, Reiländer A, Maiworm M, Baudrexel S, Meuth S, Rosenow F, Steinmetz H, Wagner M, et al. Multiparametric quantitative MRI in neurological diseases. *Front Neurol*. 2021:12:1–8. https://doi.org/10.3389/fneur.2021.640239.

Simpson LA, Eng JJ, Hsieh JTC, Wolfe and the Spinal Cord Injury Re DL. The health and life priorities of individuals with spinal cord injury: a systematic review. *J Neurotrauma*. 2012:29(8):1548–1555. https://doi.org/10.1089/neu.2011.2226.

Song S-K, Sun S-W, Ramsbottom MJ, Chang C, Russell J, Cross AH. Dysmyelination revealed through MRI as increased radial (but unchanged axial) diffusion of water. *NeuroImage*. 2002:17(3):1429–1436. https://doi.org/10.1006/nimg.2002.1267.

Song S-K, Sun S-W, Ju W-K, Lin S-J, Cross AH, Neufeld AH. Diffusion tensor imaging detects and differentiates axon and myelin degeneration in mouse optic nerve after retinal ischemia. *NeuroImage*. 2003:20(3):1714–1722. https://doi.org/10.1016/j.neuroimage.2003.07.005.

Streitbürger D-P, Möller HE, Tittgemeyer M, Hund-Georgiadis M, Schroeter ML, Mueller K. Investigating structural brain changes of dehydration using voxel-based morphometry. *PLoS One*. 2012:7(8):e44195, 1–8. https://doi.org/10.1371/journal.pone.0044195.

Sun S-W, Liang H-F, Trinkaus K, Cross AH, Armstrong RC, Song S-K. Noninvasive detection of cuprizone induced axonal damage and demyelination in the mouse corpus callosum. *Magn Reson Med*. 2006:55(2):302–308. https://doi.org/10.1002/mrm.20774.

Sun S-W, Liang H-F, Cross AH, Song S-K. Evolving Wallerian degeneration after transient retinal ischemia in mice characterized by diffusion tensor imaging. *NeuroImage*. 2008:40(1):1–10. https://doi.org/10.1016/j.neuroimage.2007.11.049.

Syka M, Keller J, Klempíř J, Rulseh AM, Roth J, Jech R, Vorisek I, Vymazal J. Correlation between relaxometry and diffusion tensor imaging in the globus pallidus of Huntington's disease patients. *PLoS One*. 2015:10(3):1–14. https://doi.org/10.1371/journal.pone.0118907.

Takeuchi H, Sekiguchi A, Taki Y, Yokoyama S, Yomogida Y, Komuro N, Yamanouchi T, Suzuki S, Kawashima R. Training of working memory impacts structural connectivity. *J Neurosci*. 2010:30(9):3297–3303. https://doi.org/10.1523/JNEUROSCI.4611-09.2010.

Taubert M, Draganski B, Anwander A, Muller K, Horstmann A, Villringer A, Ragert P. Dynamic properties of human brain structure: learning-related changes in cortical areas and associated fiber connections. *J Neurosci*. 2010:30(35):11670–11677. https://doi.org/10.1523/JNEUROSCI.2567-10.2010.

Taubert M, Lohmann G, Margulies DS, Villringer A, Ragert P. Long-term effects of motor training on resting-state networks and underlying brain structure. *NeuroImage*. 2011:57(4):1492–1498. https://doi.org/10.1016/j.neuroimage.2011.05.078.

Taubert M, Mehnert J, Pleger B, Villringer A. Rapid and specific gray matter changes in M1 induced by balance training. *NeuroImage*. 2016:133:399–407. https://doi.org/10.1016/j.neuroimage.2016.03.017.

Theodosis DT, Poulain DA, Oliet SHRR. Activity-dependent structural and functional plasticity of astrocyte-neuron interactions. *Physiol Rev*. 2008:88(3):983–1008. https://doi.org/10.1152/physrev.00036.2007.

Thomas AG, Dennis A, Rawlings NB, Stagg CJ, Matthews L, Morris M, Kolind SH, Foxley S, Jenkinson M, Nichols TE, et al. Multi-modal characterization of rapid anterior hippocampal volume increase associated with aerobic exercise. *NeuroImage*. 2016:131:162–170. https://doi.org/10.1016/j.neuroimage.2015.10.090.

Toscano-Silva M, da Silva SG, Scorza FA, Bonvent JJ, Cavalheiro EA, Arida RM. Hippocampal mossy fiber sprouting induced by forced and voluntary physical exercise. *Physiol Behav*. 2010:101(2):302–308. https://doi.org/10.1016/j.physbeh.2010.05.012.

Tran PV, Kennedy BC, Lien YC, Simmons RA, Georgieff MK. Fetal iron deficiency induces chromatin remodeling at the Bdnf locus in adult rat hippocampus. *Am J Physiol Regul Integr*

Comp Physiol. 2015:308(4):R276–R282. https://doi.org/10.1152/ajpregu.00429.2014.

Tronel S, Fabre A, Charrier V, Oliet SHR, Gage FH, Abrous DN. Spatial learning sculpts the dendritic arbor of adult-born hippocampal neurons. *Proc Natl Acad Sci USA*. 2010:107(17):7963–7968. https://doi.org/10.1073/pnas.0914613107.

van der Weijden CWJ, García DV, Borra RJH, Thurner P, Meilof JF, van Laar P-J, Dierckx RAJO, Gutmann IW, de Vries EFJ. Myelin quantification with MRI: a systematic review of accuracy and reproducibility. *NeuroImage*. 2021:226:117561. https://doi.org/10.1016/j.neuroimage.2020.117561.

van der Weijden CWJ, Biondetti E, Gutmann IW, Dijkstra H, McKerchar R, de Paula FD, de Vries EFJ, Meilof JF, Dierckx RAJO, Prevost VH, et al. Quantitative myelin imaging with MRI and PET: an overview of techniques and their validation status. *Brain*. 2023:146(4):1243–1266. https://doi.org/10.1093/brain/awac436.

Wang B, Fan Y, Lu M, Li S, Song Z, Peng X, Zhang R, Lin Q, He Y, Wang J, et al. Brain anatomical networks in world class gymnasts: a DTI tractography study. *NeuroImage*. 2013:65:476–487. https://doi.org/10.1016/j.neuroimage.2012.10.007.

Weiskopf N, Edwards LJ, Helms G, Mohammadi S, Kirilina E. Quantitative magnetic resonance imaging of brain anatomy and in vivo histology. *Nat Rev Phys*. 2021:3(8):570–588. https://doi.org/10.1038/s42254-021-00326-1.

Wenger E, Kühn S, Verrel J, Mårtensson J, Bodammer NC, Lindenberger U, Lövdén M. Repeated structural imaging reveals nonlinear progression of experience-dependent volume changes in human motor cortex. *Cereb Cortex*. 2016:27(5):bhw141–bh2925. https://doi.org/10.1093/cercor/bhw141.

Weston PSJ, Simpson IJA, Ryan NS, Ourselin S, Fox NC. Diffusion imaging changes in grey matter in Alzheimer's disease: a potential marker of early neurodegeneration. *Alzheimers Res Ther*. 2015:7(1):47. https://doi.org/10.1186/s13195-015-0132-3.

Whitwell JL, Avula R, Senjem ML, Kantarci K, Weigand SD, Samikoglu A, Edmonson HA, Vemuri P, Knopman DS, Boeve BF, et al. Gray and white matter water diffusion in the syndromic variants of frontotemporal dementia. *Neurology*. 2010:74(16):1279–1287. https://doi.org/10.1212/WNL.0b013e3181d9edde.

Xie M, Wang Q, Wu T-H, Song S-K, Sun S-W. Delayed axonal degeneration in slow Wallerian degeneration mutant mice detected using diffusion tensor imaging. *Neuroscience*. 2011:197:339–347. https://doi.org/10.1016/j.neuroscience.2011.09.042.

Yang G, Pan F, Gan W-B. Stably maintained dendritic spines are associated with lifelong memories. *Nature*. 2009:462(7275):920–924. https://doi.org/10.1038/nature08577.

Yasuda M, Johnson-Venkatesh EM, Zhang H, Parent JM, Sutton MA, Umemori H. Multiple forms of activity-dependent competition refine hippocampal circuits in vivo. *Neuron*. 2011:70(6):1128–1142. https://doi.org/10.1016/j.neuron.2011.04.027.

Yeung MSY, Zdunek S, Bergmann O, Bernard S, Salehpour M, Alkass K, Perl S, Tisdale J, Possnert G, Brundin L, et al. Dynamics of oligodendrocyte generation and myelination in the human brain. *Cell*. 2014:159(4):766–774. https://doi.org/10.1016/j.cell.2014.10.011.

Zatorre RJ, Fields RD, Johansen-Berg H. Plasticity in gray and white: neuroimaging changes in brain structure during learning. *Nat Neurosci*. 2012:15(4):528–536. https://doi.org/10.1038/nn.3045.

Zhang J, Jones M, DeBoy CA, Reich DS, Farrell JAD, Hoffman PN, Griffin JW, Sheikh KA, Miller MI, Mori S, et al. Diffusion tensor magnetic resonance imaging of Wallerian degeneration in rat spinal cord after dorsal root axotomy. *J Neurosci*. 2009:29(10):3160–3171. https://doi.org/10.1523/JNEUROSCI.3941-08.2009.

Ziegler G, Grabher P, Thompson A, Altmann D, Hupp M, Ashburner J, Friston K, Weiskopf N, Curt A, Freund P. Progressive neurodegeneration following spinal cord injury: implications for clinical trials. *Neurology*. 2018:90(14):e1257–e1266. https://doi.org/10.1212/WNL.0000000000005258.